Automation and investigation of scandium separation from ionic contaminants using ion-exchange chromatography and electrochemical methods

Rudolfs Janis Zabolockis*

*University of Latvia, Institute of Chemical Physics, 1 Jelgavas street, LV-1004, Riga, Latvia
CERN Summer Student Program, SY-STI-RBS, July 3rd – September 8th 2023
Supervisors: Laura Lambert & Edgars Mamis
rudolfs_janis.zabolockis@lu.lv
08.09.2023.

ABSTRACT

Scandium radioisotopes can be used to perform diagnostics (positron emission tomography and single-photon emission computer tomography) and therapy on patients (theranostics) due to low toxicity, short half-lives, and stable decay products. $^{43,\ 44}$Sc and ^{47}Sc can be produced from elements such as Ca, V, Ti by protons irradiation.

CERN MEDICIS facility can irradiate target materials with a proton beam of 1.4 GeV and off-line separate the produced mixture elements/isotopes by using a mass separation device. Samples which are collected on Al or Zn coated Au foils (alternatively – NaCl coated Al) still contain isobaric contaminants that have to be separated by chemical methods.

In this document the update of methods and results of scandium (stable and radioactive) separation from contaminants are reported including a novel method of removing impurities by aqueous electrolysis of Sc/ impurity mixtures. Sample investigation has been conducted with ICP-MS PLASMAQUANT, XRF ThermoScientific Niton XL3t, SEM-FIB Zeiss XB 540, current, voltage, and temperature registration using Keithly 2000 multimeters. Radiation measurements conducted with Canberra Cryo-Pulse 5 plus GX4020 gamma spectroscope and radiameter ThermoScientific FH 40G-L10. A proposed schematic for an automized system shown as well as tests for a semi-automated system successfully completed. Electrochemical separation method shows application in contaminant removal (in aqueous media). ^{47}Sc separation recoverability using ion-exchange DGA resin shows 81.4 ± 13.2 % for 3 mm Diba Omnifit Benchmark Microbore column and 75.9 ± 11.8 % for 5 mm Diba Omnifit EZ adjustable end-piece column. The actual radiochemical recoverability is estimated to be ~ 99.9 % (~ 95% if accounting for 5 - 6% left in Al foil bulk due to implantation).

TABLE OF CONTENTS

INTRODUCTION

CERN MEDICIS (MEDical Isotopes Collected from ISolde) (see Fig. 1) is a research facility that focuses on the methodology of production and research of medically relevant isotopes such as $^{43, 44, 47}$Sc, ^{103}Pd, ^{111}Ag, ^{128}Ba, ^{155}Tb, $^{165, 167}$Tm, ^{199}Au, $^{225, 227}$Ac, and others [1].

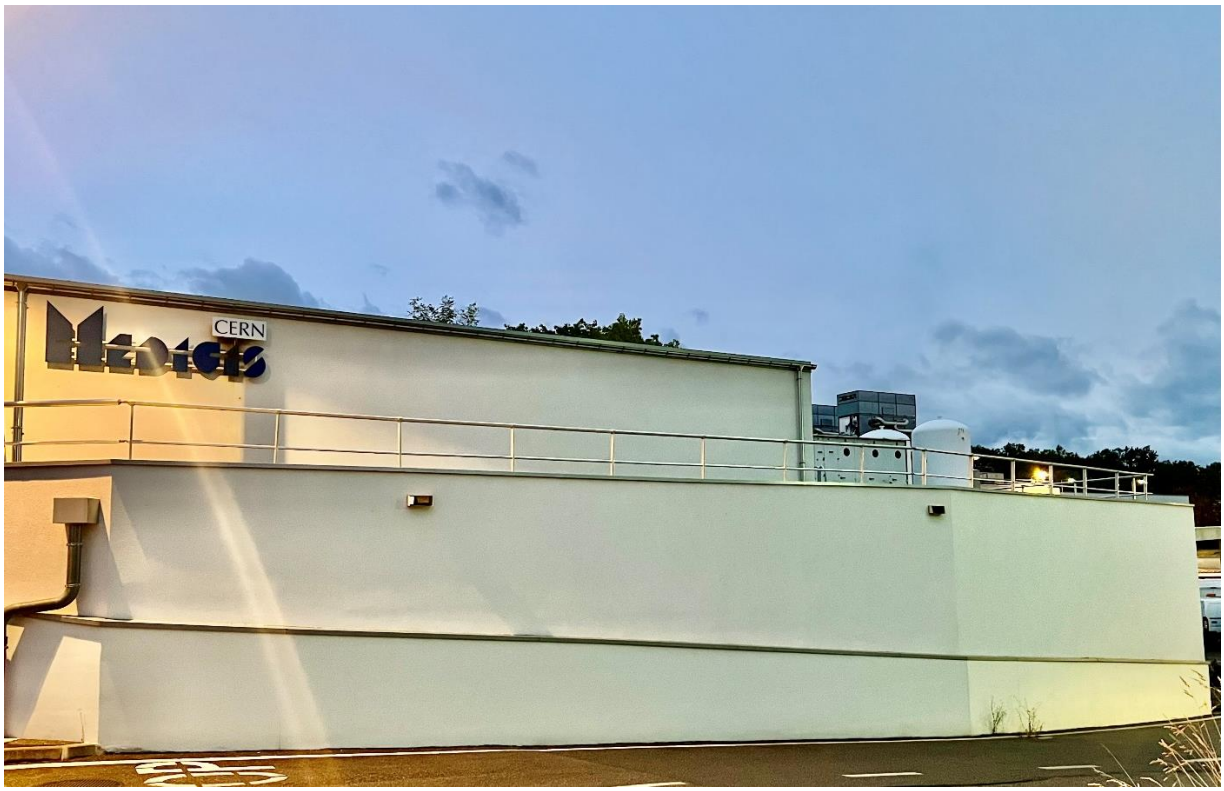

Fig. 1. **CERN MEDICIS facility, Esplanade des Particules 1, Meyrin, Switzerland**

Of the listed isotopes, Sc isotopes are of high interest due to the application in theranostics (a combination of therapy and diagnostics) due to positron emission ($^{43, 44}$Sc) due to p>n and electron emission for ^{47}Sc due to n>p (for decay schemes see Fig. 2).

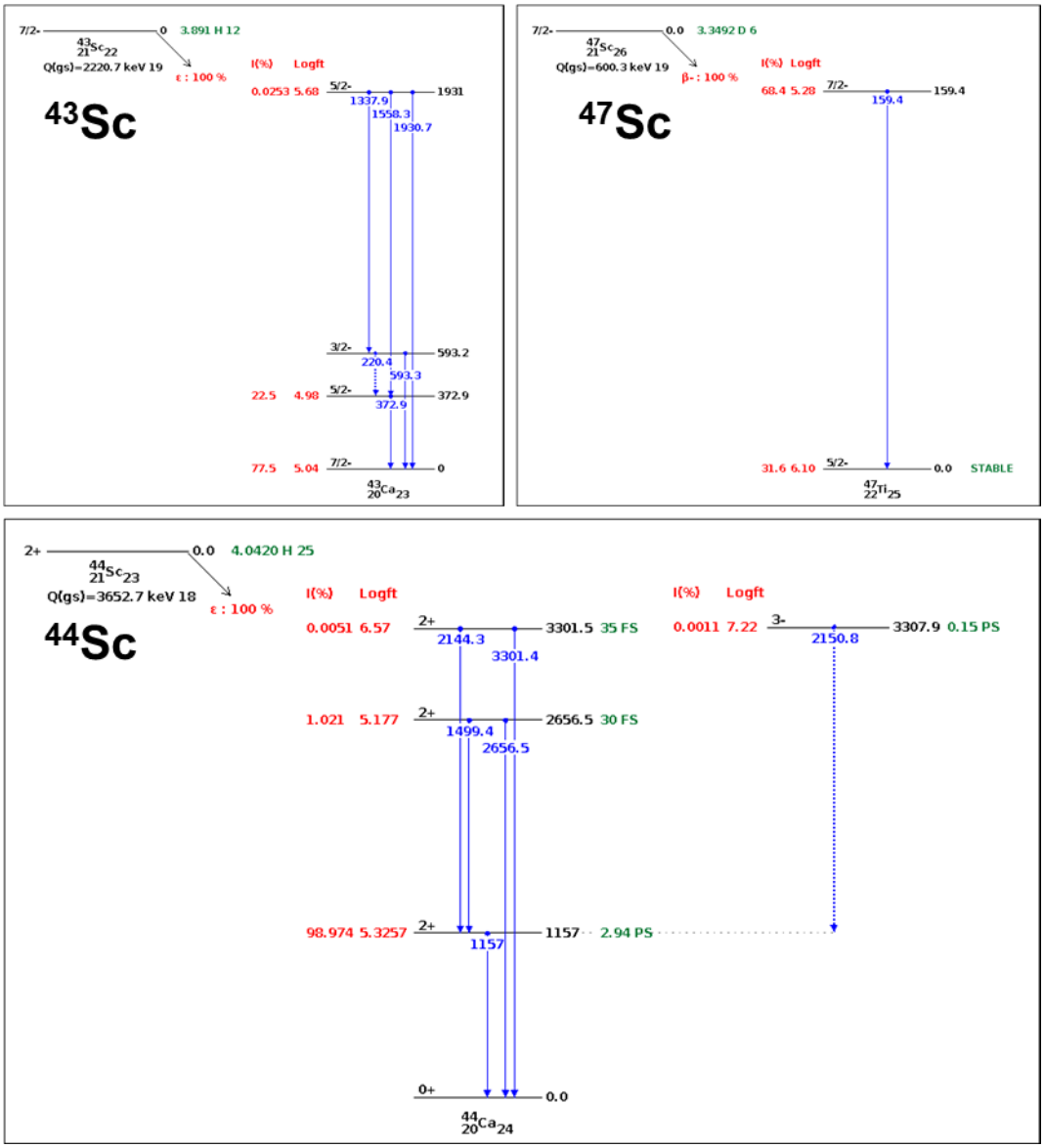

Fig. 2. **^{43,44}Sc and ^{47}Sc decay schemes** [2–4]

Therefore, **^{43}Sc** and **^{44}Sc** can be used in **positron emission tomography** (PET) to detect and measure physiological processes in the body and illnesses such as cancer. PET is based on the emission of 2 back-to-back gamma rays due to the annihilation of a positron (β^+) interacting with the antiparticle – an electron – in the body.

^{47}Sc is a β^- (100%; E_{max} = 162 keV, E_{avg} = 109 keV) and γ (68.3%; E = 159.4 keV, E_{avg} = 109 keV) emitter, therefore, can be used both for **therapeutic applications** (β^-) and in **single-photon emission computer tomography** (SPECT) due to the emission of a photon undergoing β^- decay.

Such radioisotopes can be produced by the interaction of protons with materials such as titanium, vanadium, and calcium. The production of Sc isotopes in CERN takes place in CERN MEDICIS using 1.4 GeV accelerated protons provided from the CERN proton synchrotron booster (PSB) in collaboration with CERN Isotope Separator On-Line DEvice (ISOLDE). ISOLDE experiment absorbs only 10 % of the total proton beam from PSB letting through the rest of the proton beam to irradiate MEDICIS targets (see Fig. 3) [5].

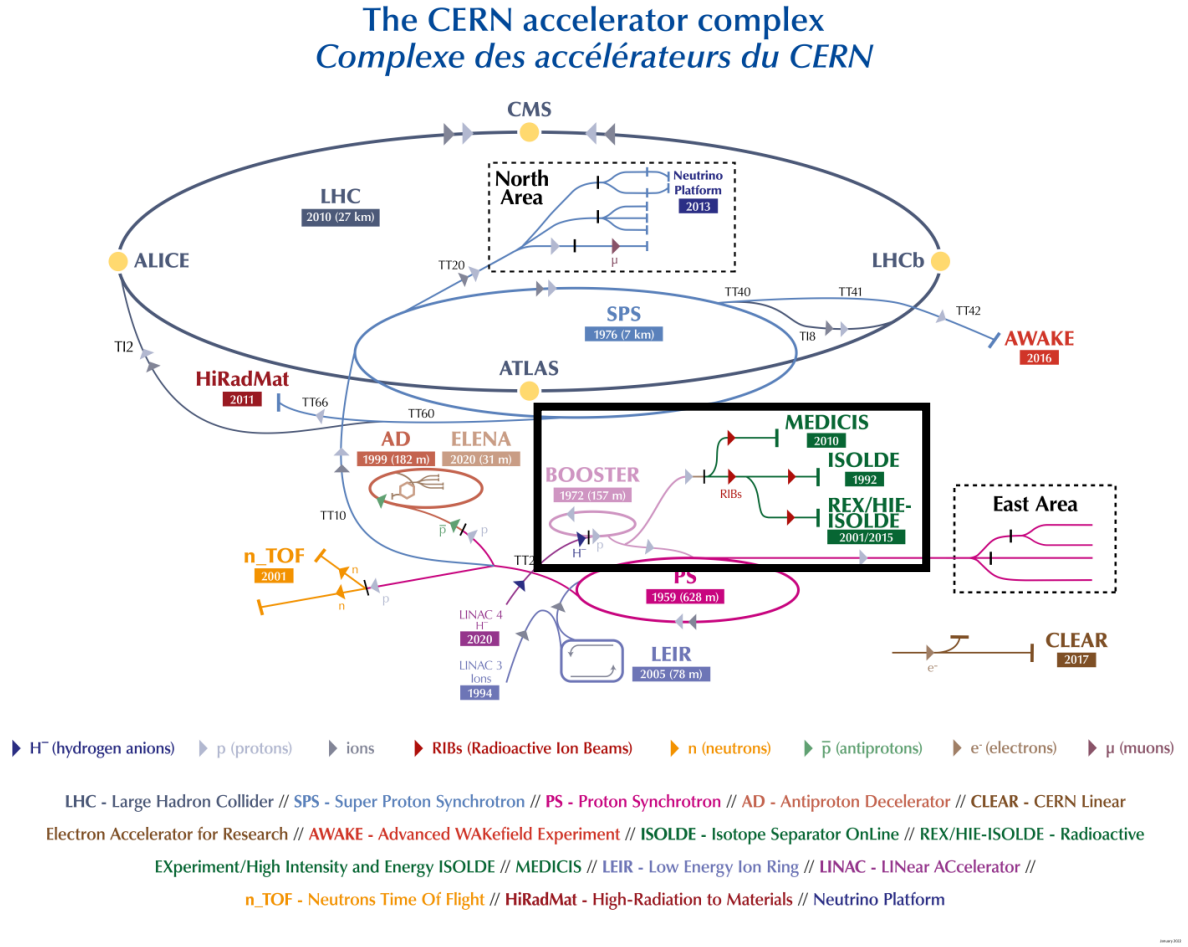

Fig. 3. **CERN accelerator complex with ISOLDE-MEDICIS connection highlighted in black** [6]

The materials relevant for isotope such as $^{43,\ 44}$Sc and ^{47}Sc production are placed inside a target – a specifically designed vessel constructed primarily of tantalum that can facilitate pressure of 10^{-6} mbar and temperatures more than 2000 ^{o}C. The material-loaded target is irradiated by 1.4 GeV protons at CERN ISOLDE receiving 90% of the proton beam, placed directly behind ISOLDE targets.

After irradiation, the targets are taken by a robot (KUKA, Germany) to an off-line (mass separation is not happening simultaneously with proton irradiation) mass separator unit in MEDICIS (Fig. 4).

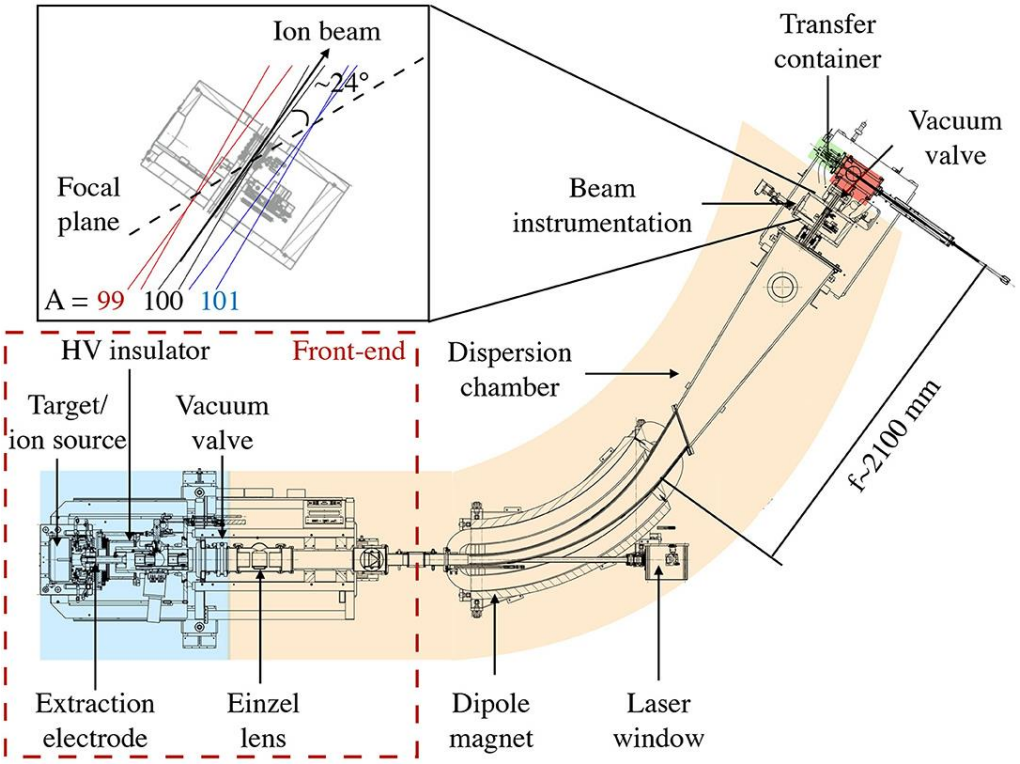

Fig. 4. **CERN MEDICIS off-line facility mass separator unit** [5]

The off-line unit in MEDICIS consists of the proton irradiated target and ion source. The target container features a tantalum tubular oven with Ø 2 cm and length of 20 cm which is connected to an ion source by a transfer line. The ionization unit is a cylindric device made from tantalum, rhenium, or tungsten with Ø 3 mm and length of 34 mm, as per ISOLDE standard.

The target is held at a high potential (up to 65 kV) in a distance of 50 to 100 mm (acceleration gap) from a ground-potential extraction electrode. The ion beam is then shaped by an einzel lens (three cylindrical apertures, 20 mm in between each, two side apertures held at ground potential). Additional auxiliary equipment/systems such as X-Y electrostatic deflectors correct the beam to the focal plane, the vacuum system allows to achieve pressure of 10^{-5} to 10^{-7} mbar, a gas leak adds possibility to introduce gas into the system, and a MEdicis Laser Ion Source Setup At CERN (MELISSA) added in 2019 gives the possibility to ionize a specific element thus facilitating isobar separation. [5]

Mass separation according to ion mass/charge value (due to Lorentz force) is achieved by a 55° double-focusing dipole magnet (provided from KU Leuven, Belgium) with a bending radius of 1.5 m, water cooled. [5]

Faraday cups (before the magnet and after) are used to measure ion beam current. Wire scanners allow to see the beam path and to optimize the beam parameters for the focal plane and focus the beam. A collimator, slits and electron deflectors are placed directly before the collection point.

The collection point is usually on a metallic foil placed into a sample holder facilitating up to three samples. The foils are usually Al or Zn coated gold (1.5 x 2.5 cm). Variations such as salt foils (NaCl layer on Al substrate) have also been used. [7]

Once the isotope of interest (e.g., ^{47}Sc) is collected using molecular beams consisting of species such as ScF_2^+, ScF^+ and others produced by Sc reaction with fluorine-containing compounds (e.g., CF_4) and further ionization, it must be separated from isobaric contaminants of elements like ^{47}Ti, ^{47}Ca, ^{47}V and others with molecules of same mass that are incompatible with further usage in a medical application.

1. THEORETICAL

In the theoretical part both the electrochemical and ion exchange methods have been explained and the method-specific advantages and challenges identified from a theoretical aspect.

1.1. Electrochemical separation

The electrochemical method described in this document supplies the means of separating Zn, V, and somewhat Ti contaminants from Sc-containing aqueous samples. The electrochemical method described here using aqueous solutions should be used in conjuncture with ion-exchange chromatography due to water electrolysis potential limit (thermodynamical H_2O electrolysis potential 1.23 V [8], and 1.8-2.0 V due to overpotential [9].

This electrochemical separation method is based on the fundamental electrochemical properties of metals. Similar methods have separately been used to isolate various different metallic elements in both aqueous and non-aqueous media. [10–14]

Standard reduction potentials for metals of interest can be seen in Table No. 1

Table No. 1. **Some metal standard reduction potentials**

Element	Reduction half reaction	Standard reduction potential [$E^{\ominus}$], V	Literature reference
Zn	$Zn^{2+}_{(aq)} + 2\,e^- \rightleftharpoons Zn_{(s)}$	-0.7618	[15]
V	$V^{2+}_{(aq)} + 2\,e^- \rightleftharpoons V_{(s)}$	-1.13	[16]
Ti	$Ti^{3+}_{(aq)} + 3\,e^- \rightleftharpoons Ti_{(s)}$	-1.37	[17]
Al	$Al^{3+}_{(aq)} + 3\,e^- \rightleftharpoons Al_{(s)}$	-1.662	[16]
Sc	$Sc^{3+}_{(aq)} + 3\,e^- \rightleftharpoons Sc_{(s)}$	-2.007	[16]
Na	$Na^{+}_{(aq)} + e^- \rightleftharpoons Na_{(s)}$	-2.71	[8]
Ca	$Ca^{2+}_{(aq)} + 2\,e^- \rightleftharpoons Ca_{(s)}$	-2.868	[8]
Rb	$Rb^{+}_{(aq)} + e^- \rightleftharpoons Rb_{(s)}$	-2.98	[8]

From Table No. 1, the redox potentials of almost all metals are higher than Sc and the properties of these metals allow them to be deposited on an electrode (up to a certain efficiency) during electrolysis. The selectivity of deposition is due to the difference in redox potentials – applying up to 2 V DC should deposit Zn, Ti, and V

on the negative electrode – cathode. The temperature of the electrolysis bath affects the achievable current as the temperature is proportional to ion mobility (activity) in solution. The higher the temperature, the more current can be expected should two baths of the same composition be compared. It must be mentioned that after 60 °C water starts to evaporate quickly [18] which is not preferable for the process (dry flaking of salts on electrode, loss of conducting solvent, radiological risks, etc.). It is expected that the following reactions take place to some extent during the electrolysis of solutions containing Sc, H Zn, Ti, V, Al, Ca, Na and Rb metal cations:

$$Zn^{2+}_{(aq)} + 2\,e^- \rightarrow Zn_{(s)} \downarrow$$
$$V^{2+}_{(aq)} + 2\,e^- \rightarrow V_{(s)} \downarrow$$
$$Ti^{3+}_{(aq)} + 3\,e^- \rightarrow Ti_{(s)} \downarrow$$

As the voltage is raised above 1.23 V, the possibility of water electrolysis should be considered [19]:

$$2\,H_2O\, - 4\,e^- \rightleftharpoons O_{2(g)} + 4\,H^+_{(aq)}$$
$$2\,H_2O + 2\,e^- \rightleftharpoons H_{2(g)} + 2\,OH^-_{(aq)}$$

However, due to the overpotential of the hydrogen evolution reaction it can be estimated that the rate of H_2 and O_2 evolution under electrolysis conditions (1.8 CV DC; up to 0.004 A; average 0.002 A) the total amount of hydrogen generated would not exceed 0.0003 mol (volume at standard conditions 6 mL) at a maximum rate of H_2 evolution 1 mL/h or ~0.02 mL/min as per the calculations stated below (Equations 1-4):

$$Q = \int_{t=0}^{t=x} I(t)dt = 52.68\,C \quad (1)$$

$$n = \frac{Q}{z \cdot F} = \frac{52.68C}{2 \cdot 96485.3C/mol} = 0.000273\,mol \sim 0.0003\,mol \quad (2)$$

$$V = n \cdot V_o = 0.0003mol \cdot 22.4L/mol = 0.0061L = \sim 6\,mL \quad (3)$$

$$\vartheta = \frac{V}{t} = \frac{0.0061L \cdot 1000}{25195s/3600} = \sim 1\,mL/h \quad (4)$$

where *Q – total charge [C], n – amount of substance [mol], t – time [s], I – current [A], V – volume [L], z – number of electrons, V_o – normal volume [L/mol] (approx. 22.4 L/mol), ϑ – rate of gas evolution [mL/h].*

It must be noted that the experiment is executed in a fume hood with adequate ventilation and the electrolysis cell is open to the surrounding air with no possibility of gas pocket formation. Assuming the Lower Explosive Limit (LEL) for H_2 to be 4% [20], it can be calculated that even if the whole amount of H_2 produced would be released instantaneously (0.0003 mol), supposing a fume hood (no ventilation considered for calculation) 1 m wide, 1 m high and with depth of 0.5 m would reach H_2 content of 0.0012 % which is three orders of magnitude less than the LEL.

The formation of gaseous chlorine on the anode (+) is anticipated depending on the electrolysis bath contents as the oxidation potential for 2 Cl^-/Cl_2 is -1,37 V:

$$2\,Cl^-_{(aq)} - 2\,e^- \rightleftharpoons Cl_{2\,(g)}$$

Total volume could be at the most 12 mL of Cl_2 at a maximum release rate of 1.7 mL/h or 0.03 mL/min which should at once dissolve in solution as Cl_2 is soluble in H_2O (at 50 °C 4 g Cl_2 dissolves in 1 kg of H_2O [21]). Calculating from the total amount of Cl_2, the mass concentration would be 3.8 g Cl_2/ kg H_2O, below the threshold where it would escape into the atmosphere as a gas.

Should a non-aqueous bath be used (e.g., ethanol) no water electrolysis reaction would impede the deposition of metals and as long as the reduction potentials in ethanol or other non-aqueous solution are known, the metals could be deposited with up to 100 % efficiency. [12,13]

1.2.Ion-exchange chromatography separation

Ion-exchange chromatography [22] works by first adsorbing the ion of interest inside a chromatographic column on a resin (loading phase), following the washing of the column to flush out any contaminants present (feed through phase). Then an appropriate eluting agent is used (product ion elution phase) followed by a flushing

with deionized water to remove all ions from the column. The resin can then be regenerated and reused.

Various types of resin for ion exchange chromatography are known [23–27] For Sc the best type of resin has been determined to be 2,2′-oxybis(N,N-dioctlyacetamide) or DGA for short. The structural formula for the DGA resin is shown in Fig. 5.

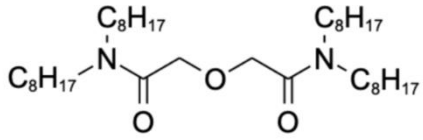

2,2'-oxybis(*N*,*N*-dioctylacetamide)

Fig. 5. **DGA resin structural formula (non-branched)**

The DGA resin interacts with Sc^{3+} ions by forming micelle type non-covalent complexes, 3 DGA molecules per metal ion according to the mechanism:

$$Sc^{3+}_{(aq)} + 3DGA_{(org)} + 3NO_3^- \rightarrow [Sc(DGA)_3(NO_3)_3]_{(org)}$$

The coordination complex (micelle) can then be broken down by using an eluting agent (usually 0.1 M HCl).

DGA resin chromatography parameters have been reported in depth by [25,28].

Regarding mobile phase and eluent concentrations, the best results were achieved using 2.5 M HNO_3 and 0.1 M HCl [25]. The method using DGA resin for Sc separation has been reported also by P. Kalnina [29].

The best results were achieved using 0.5 mL/min flow rate, 3 mm inner diameter column, 70 mg of DGA branched resin. Separation efficiency for was reported as 88 ± 3 %. [24,25,28]

2. EXPERIMENTAL

The experimental section features the methods, materials, devices and samples for ion-exchange chromatography and electrochemical ion separation from Sc containing samples as well as the complete procedure for each.

2.1. Electrochemical method

The electrochemical method was developed in order to increase the ion-exchange chromatography efficiency by removing at least partially if not fully the contaminant ions like V^{2+}, Ti^{3+} and Zn^{2+}.

2.1.1. Materials and equipment used

For aqueous electrolysis of metallic ion solutions (Sc, Zn, Ti, V, Al, Ca, Na and Rb) the following equipment/ materials were used:

1. DC power source ISO-TECH IPS 4303, 0-30 V, 3 A;
2. Electrodes – graphite, Ø 0.58 ± 0.02 mm, custom made at CERN (B. Crepieux);
3. Connecting wires;
4. Glass sample vial, 20 mL, PerkinElmer;
5. Laboratory stand and holders for electrodes (insulated);
6. Electric hotplate with magnetic stirring IKA RET Basic 0-340 ^{o}C, 0-1700 rpm;
7. Stirrbar (agitator);
8. Keithly 2000 multimeter (for current and temperature acquisition);
9. Type-K thermocouple;
10. Fume hood;
11. Analytical balance Pioneer, 0.0000 – 210.0000 g, ± 0.0001 g;
12. Automatic pipettes (10.0 ± 0.2 μL, 1000 ± 20 μL, 5000 ± 100 μL, and 10.00 ± 0.02 mL) and tips;
13. Deionized water (0.055 μS/cm);
14. Personal protective equipment (PPE) such as gloves;
15. ICP-MS standards of Sc, Zn, Ti, V, Al, Ca, Na and Rb ions, 1000 mg/L;
16. Hydrochloric acid, 37%, ACS reagent grade, Sigma Aldrich
17. Nitric acid 70%, ACS reagent grade, Sigma Aldrich
18. Volumetric flasks, 10.00 ± 0.02 mL; 25.00 ± 0.04 mL; 50.00 ± 0.06 mL; 100.0 ± 0.1 mL;

19. Inductively-coupled mass spectrometer (ICP-MS) PLASMAQUANT, Analytik Jena, software – ASPECT MS;
20. Radiameter ThermoScientific FH 40G-L10 (10 nSv/h – 100 mSv/h; 30 keV – 4.4 MeV);
21. Gamma spectrometer Canberra Cryo-Pulse 5 plus GX4020, bias voltage 3.5 kV, Apex gamma software, detection limit for ^{47}Sc: 302 Bq.
22. X-ray fluorescence detector (XRF) ThermoScientific Niton XL3t, up to 40 keV, precious metal library;
23. Focused ion beam scanning electron microscope (FIB-SEM) Zeiss XB 540, FIB performance: Ga-Ion, 3 nm at 30 kV, 300 – 500,000 x magnification, SEM performance – 0.7 nm at 30 kV, $U_{acc.}$ = 0.02 – 30 kV, magnification 12 – 2,000,000 x.

2.1.2. ^{45}Sc electrochemical separation (stable) tests

The testing procedure was as follows:

1. Preparation of ion mixture from ICP-MS (Inductively Coupled Mass Spectrometry) standards and sample naming (ES *X* where *X* is the number of the experiment);
2. Drawing 5 mL of sample (ES *X* STD where STD means standard) for ICP-MS analysis;
3. Inserting graphite electrodes into the solution, connecting wires to cathode and anode;
4. Electrolysis at 1.8 V, recording of current by time, heating (optional) and stirring;
5. Extraction of electrodes from solution while electric potential is still applied;
6. Potential removed and electrodes rinsed with deionized water into sample vial;
7. Contents of sample vial quantitatively transferred to volumetric flask and diluted;
8. Drawing sample (ES *X*) for ICP-MS analysis;
9. Electrodes immersed in 2 M HCl for 5 min for cleaning purposes;
10. Calculation and evaluation of acquired data.

A schematic image of the experimental setup can be seen in Fig. 6.

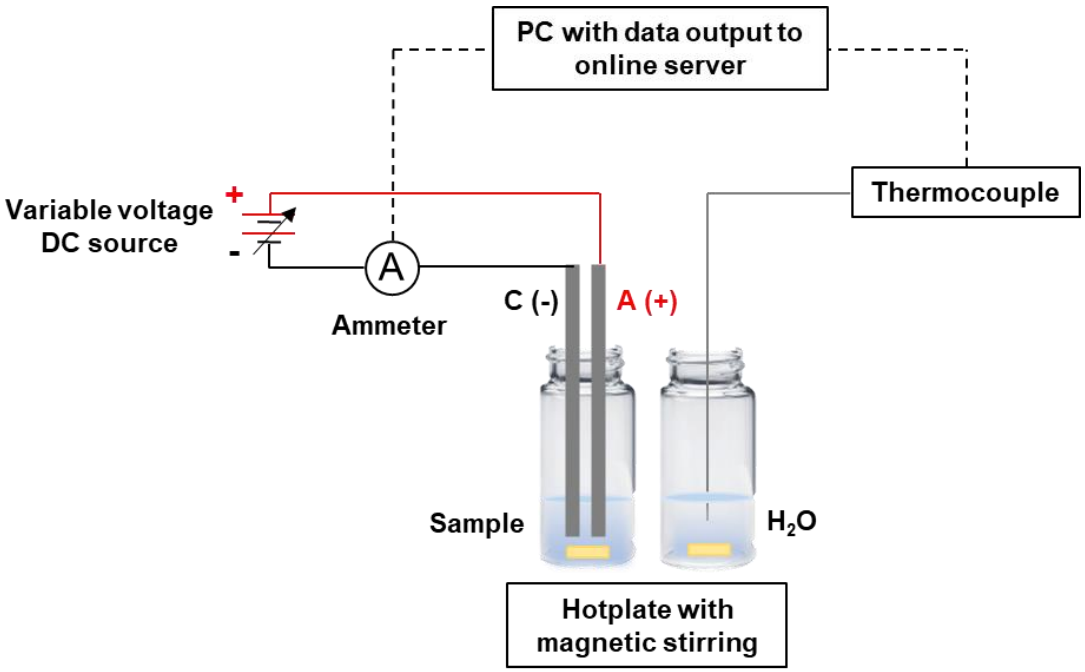

Fig. 6. **Electrochemical separation setup**

The rate of deposition on the cathode is directly proportional to the cathodic current, therefore, in cases of low electrolyte concentration (ionic strength < 1 M) to increase the current the solution is heated up to 55 °C (heating above 60 °C causes rapid evaporation) and to increase ion mobility [30]. The rate of deposition is of importance due to the radiation protection and half-life factors.

The motivation of sample composition is as follows:

- Samples ES1 and ES2 prepared per P. Kalnina's report [29], which stated 13.6 µg ^{45}Sc implanted in a foil. The mass and amount (Equation 5, 6) of Al or Zn (assuming 1.5 x 2.5 cm Au foil covered with 500 nm of Al or Zn) can be estimated knowing the density of the layer (assumed to be close to bulk metal density):

$$m = \rho \cdot x \cdot y \cdot z \cdot 10^{-7} \quad (5)$$

where *m – mass of Al or Zn coating [g], ρ – density of the layer [g/cm³], x – length of the foil [cm], y – width of the foil [cm], z – thickness of the Al or Zn layer [nm]*

$$n = \frac{m}{M} \quad (6)$$

where *n – amount of Zn or Al on the Au foil [mol], M – the molar mass of Al or Zn [g/mol].*

- Samples ES3-ES6 prepared assuming 100 MBq ^{47}Sc production on metal foil as per the calculations below (Equation 7):

$$N = \frac{A \cdot T_{1/2}}{\ln(2)} \tag{7}$$

where *N – number of atoms, A – the radioactivity of an isotope [Bq],* $T_{1/2}$ *– radioactive isotope half-life [s].*

The amount and thus mass of 100 MBq of Sc can be calculated (Equation 8):

$$m = \frac{N \cdot M}{N_A} \tag{8}$$

where *m – mass of an isotope [g], M – molar mass of the isotope [g/mol],* N_A *– Avogadro's number [1/mol].*

- Samples ES7-ES8 were prepared to simulate NaCl coated Al foil for ^{47}Sc separation using TiC as target material (NaCl mass assumed to be 0.5 g).
- ES9 was prepared for SEM-FIB analysis – to evaluate metal deposition profiles.
- ES10-11 prepared to simulate for V target material, 100 MBq ^{47}Sc.

To develop and study the method tests with ^{45}Sc and other stable metal isotopes such as Al, Ti, V, Ca, Rb, Na and Zn were conducted (see full sample itinerary in Table No. 2, continued from pages 17-18) as well as ^{47}Sc sample from NaCl coated Al foil.

Table No. 2. **Sample identification and relevant information**

Sample name	Element	Mass concentration (theoretical; before electrolysis), mg/L	Ratio to Sc	Additional info
ES1	Al	40	17	Not-deionized water (~250 μS/cm), room temperature: 29 °C
	Sc	2.4	1.0	
	Ti	0.030	$1.3 \cdot 10^{-2}$	
	V	0.030	$1.3 \cdot 10^{-2}$	
	Ca	0.030	$1.3 \cdot 10^{-2}$	
ES2	Al	40	17	Not-deionized water (~250 μS/cm), room temperature: 24 °C
	Sc	2.4	1.0	
	Ti	0.030	$1.3 \cdot 10^{-2}$	
	V	0.030	$1.3 \cdot 10^{-2}$	
	Ca	0.030	$1.3 \cdot 10^{-2}$	
ES3	Ti	330	$1.0 \cdot 10^{6}$	3 mL 12.1 M HCl, room temperature: 21 °C
	Al	24	$7.3 \cdot 10^{4}$	
	Sc	0.00033	1.0	
	Ca	0.00026	0.8	
ES4	Ti	330	$1.0 \cdot 10^{6}$	2.1 mL 12.1 M HCl, 45 °C, stirring
	Al	24	$7.3 \cdot 10^{4}$	
	Sc	0.00033	1.0	
	Ca	0.00026	0.8	
ES5	Ti	330	$1.0 \cdot 10^{6}$	2.1 mL 12.1 M HCl, 30-55 °C, stirring, after electrolysis re-diluted to 10 mL
	Al	24	$7.3 \cdot 10^{4}$	
	Sc	0.00033	1.0	
	Ca	0.00026	0.8	
ES6	Ti	0.40	0.14	2.1 mL 12.1 M HCl, 55 °C, stirring
	Zn	71	25	
	Sc	2.8	1.0	
	Ca	0.00026	$1.1 \cdot 10^{-4}$	
ES7	Na	100000	$3.6 \cdot 10^{4}$	For ^{47}Sc collection test. 55 °C Ti target
	Sc	2.8	1.0	
	Al	0.40	0.14	
	Ti	0.40	0.14	
	Rb	0.030	$1.1 \cdot 10^{-2}$	
	V	0.030	$1.1 \cdot 10^{-2}$	

Sample name	Element	Mass concentration (theoretical; before electrolysis), mg/L	Ratio to Sc	Additional info
ES8	Na	100000	$5.0 \cdot 10^6$	For ^{47}Sc collection test. 55 ^{o}C Ti target
	Sc	2.8	1.0	
	Al	0.40	20	
	Ti	0.40	20	
	Rb	0.030	20	
	V	0.030	$2.0 \cdot 10^3$	
ES9	Sc	40	1.0	For FIB-SEM analysis – deposition profiles
	Al	20	0.5	
	Ti	24	0.6	
	Zn	40	1.0	
	V	2.0	$5.0 \cdot 10^{-2}$	
ES10	Na	100000	$5.0 \cdot 10^6$	For ^{47}Sc collection simulation (scaled up): V target. Trying to remove contaminants and afterwards Sc
	Sc	0.020	1.0	
	Al	0.40	20	
	Ti	0.40	20	
	Rb	0.40	20	
	V	40	$2.0 \cdot 10^3$	
ES11	Na	100000	$5.0 \cdot 10^6$	For ^{47}Sc collection simulation (scaled up): V target. Only contaminant ion removal
	Sc	0.020	1.0	
	Al	0.40	20	
	Ti	0.40	20	
	Rb	0.40	20	
	V	40	$2.0 \cdot 10^3$	
ES12	Na	100000	$5.0 \cdot 10^6$	For ^{47}Sc collection simulation (scaled up): V target. Only contaminant ion removal
	Sc	0.020	1.0	
	Al	0.40	20	
	Ti	0.40	20	
	Rb	0.40	20	
	V	40	$2.0 \cdot 10^3$	
ES13	Ti	0.40	0.14	2.1 mL 12.1 M HCl, 55 ^{o}C, stirring
	Zn	71	25	
	Sc	2.8	1.0	
	Ca	0.00026	$1.1 \cdot 10^{-4}$	

2.1.3. Electrode surface platinum plating

The electrodes used for ES1-ES11 were found to be rather porous (see Result section), therefore, both the anode cathode was covered with a layer of metallic Pt. The platinum plating was carried out using $PtCl_2$ which was reacted with concentrated HCl and then diluted:

$$PtCl_{2(s)} + 2\,HCl_{(aq)} \rightarrow H_2[Pt(Cl)_4]_{(aq)}$$

After dilution the anode and cathode were placed in the electroplating bath (identical design to Fig. 6). Due to excess HCl, Cl_2 gas was evolved on the anode during electrolysis, forming hexachloroplatinic acid (it must be noted that no heating should be used both to preserve the graphite electrodes from oxidation as well as not to decrease the solubility of Cl_2 for safety and chemical reaction reasons):

$$H_2[Pt(Cl)_4]_{(aq)} + Cl_{2(aq)} \rightarrow H_2[Pt(Cl)_6]_{(aq)}$$

Pt redox potential for hexachloroplatinic acid is 0.4 V [31], however, to achieve faster deposition, 1.4 V (below water electrolysis potential) was used, $Pt_{(s)}$ was deposited on the cathode:

$$H_2[Pt(Cl)_6]_{(aq)} \xrightarrow{electrolysis} Pt_{(s)}\ (cathode) + Cl_{2(aq)}\ (anode) + HCl_{(aq)}$$

The process was repeated switching the anode for the cathode (adding a brand-new anode) to make a platinum-plated electrode set. Platinum presence was verified with XRF measurements.

2.1.4. Mathematical calculations for electrochemical separation

The potential for ion deposition from standard conditions in aqueous solutions has been recalculated to fit the concentration and temperature of the investigated ion mixtures according to the Nernst equation (modified for metal deposition purposes by considering the acidity of the solution calculated from the added acid and the ICP-MS standard acidity), taking into consideration also the acidity of the solution (Equation 9):

$$E = E^{\ominus} - \frac{R \cdot T}{z \cdot F} \ln\left(\frac{1}{a_{A^{z+}_{(aq)}}}\right) + \frac{R \cdot T}{F} \ln\ a_{H^{+}_{(aq)}} \tag{9}$$

where E *– reduction potential at non-standard conditions depending on the concentration and acidity [V],* R *– ideal gas constant 8.314 [J/ (mol · K)],* T *– temperature of the solution [K],* z *– number of the charge in the electrochemical reaction,* F *– Faraday's constant 96485.3 [C/mol],* $a_{A^{z+}_{(aq)}}$ *– activity of metal ion* $A^{z+}_{(aq)}$ *in the solution [mol/L],* $a_{H^{+}_{(aq)}}$ *– activity of hydrogen ions in the solution [mol/L].*

Since the ionic strength in the solution is > 1 M, concentration can be approximated almost fully as the real activity of ions in the solution. [ref]

The amount of deposited metal can be calculated with Equation x and compared to the change in mass concentration given by ICP-MS results. On the time of the preparation of this report results from ICP-MS are still expected.

Since the current varies by time the total charge and thus, the amount or mass of deposited element can be calculated using an integral by time (Equation 10):

$$Q = \int_{t=0}^{t=x} I(t)dt \tag{10}$$

where Q *– total charge [C], t=0 is the start of electrolysis reaction [s], t=x is the time at which electrolysis has been stopped [s],* I *– DC current [A].*

To calculate the specific amount of each element that is deposited from the total charge, the molar fraction of each element is calculated and multiplied with the total charge (e.g., element A. See Equation 11):

$$\chi_A = \frac{n_A}{n_A + n_B + n_C + \cdots} \tag{11}$$

where χ_A *– molar fraction of a certain ion in the solution (initially),* n_A *– initial amount of A ions [mol],* n_B *– initial amount of B ions [mol],* n_C *– initial amount of C ions [mol].*

The total charge is multiplied by the molar fraction and the Faraday's law of electrolysis is solved to determine the element mass (Equation 12):

$$m_{A_{electrolysis}} = \frac{Q \cdot \chi_A \cdot M \cdot 10^3}{z \cdot F} \quad (12)$$

where m_A – *mass of element A on the electrode [mg], M – molar mass of the element A [g/mol], z – amount of charge transferred in the electrochemical deposition of A ions.*

Since the concentration of A in the initial solution and the separated (electrolyzed) solution is known from ICP-MS (Equation 13):

$$m_{A_{ICP-MS}} = (\gamma_{A_o} - \gamma_{A_f}) \cdot V_{sample} \quad (13)$$

where $m_{A_{ICP-MS}}$ – *mass of separated element A (as per ICP-MS results) [mg],* γ_{A_o} – *mass concentration of element A in the solution before electrolysis [mg/L],* γ_{A_f} – *mass concentration of element A in the solution after electrolysis [mg/L],* V_{sample} – *volume of the sample used for electrolysis [L].*

The electrochemical separation efficiency can be calculated (Equation 14, using total charge and ICP-MS results):

$$\eta = \frac{m_{A_{electrolysis}}}{m_{A_{ICP-MS}}} \cdot 100 \quad (14)$$

where η – *electrochemical separation efficiency [%].*

2.1.5. ^{47}Sc electrochemical separation (radioactive) tests

For the radioactive isotope separation, the same materials and methods apply, however, radiation counting can be used to show where ^{47}Sc is situated. Due to the high redox potential of Sc, it can be expected that the deposition on the cathode will not be 100% or possible at all, therefore, the procedure should be as follows:

1. ^{47}Sc-containing NaCl foil is dissolved using **deionized water** (**6.875 mL**) inside a glass vial (20 mL maximum volume), adding **3.125 mL 8M HNO_3** for total concentration of HNO_3 to be **2.5 M**, placing on the hotplate, sample labeled **ERS*X*** – *X* denotates experiment number;
2. The radioactivity of the solution is measured and recorded;

3. Graphite electrodes (labeled **ERS*X* C1** and **ERS*X* A1**) and a magnetic stirrbar are put into the mixture;
4. The graphite electrodes are fixed to a known depth in the mixture (provided no physical contact between electrodes is created) by laboratory stand clamps;
5. *Keithly 2000* multimeters are connected and started to register temperature and current (data saved online on *timber.cern.ch*);
6. DC power supply connected to the electrodes using connectors;
7. A vial of **10 mL H_2O** is placed on the hotplate (**labeled H_2O**) next to the sample ERS*X*, inserting thermocouple in the H_2O vial;
8. The stirring is turned on at **600 rpm**, and *if necessary due to low ion mobility hotplate shall set to 66 ^oC (solution final temperature will be ~ 55 ^oC)*;
9. *When ~55 ^oC (most important – **constant temperature**) is achieved* **or** immediately after system setup if no heating is to be used, DC power is applied to the electrodes at **1,8 V DC**;
10. Electrolysis is conducted for **30 min**;
11. **While the 1,8 V DC is still applied**, the cathode is carefully extracted from the solution – using only non-conductive surfaces. *This step is critical not to re-dissolve the deposited ions back into the solution!*
12. Once the cathode (-) is extracted the power supply is **immediately turned off**;
13. Both the cathode and anode are extracted from the mixture and carefully rinsed with deionized water **into the ERS*X* glass vial**;
14. Radioactivity of each electrode as well as that of the solution is measured and recorded, electrodes bagged and stored accordingly;
15. **New electrodes** (**ERS*X* C2** and **ERS*X* A2** respectively) are inserted into the **ESR *X* vial**, connected as previously described (**steps 3-4**);
16. Insuring no short-circuit is possible, DC power is applied to the electrodes at **2,1 V**;
17. Electrolysis conducted for **30 minutes**;
18. **Steps 11-14 repeated**;
19. Electrodes ERS*X* C2 and ERS*X* A2 removed from vial E2, rinsing into water **into the ERS*X* glass vial**;
20. *If heating was executed*, hotplate heating turned off, stirring optional to let the ESR*X* cool to room temperature;
21. All equipment unplugged from the 220 V outlets;
22. Two (2) vials collected in total – ESR*X* and ES2. In total, four (4) electrodes collected, assessed for contamination; All other equipment assessed for contamination;

23. Ion-exchange chromatography further conducted as per chapter 2.2.;
24. Gamma spectrometry measurement used to assess the activity on electrodes, solutions, and equipment (if necessary).

Due to the short half-life of ^{47}Sc a correction to gamma spectrometry measurements was made (Equation 15):

$$A_t = A_o \cdot e^{-\frac{ln2}{T_{1/2}} \cdot t} \quad (15)$$

where A_t – *the radioactivity of an isotope after an amount of t time has passed [Bq],* A_o – *initial radioactivity of the isotope at t = 0 s [Bq],* $T_{1/2}$ – *radioactive isotope half-life [s], t – amount of time which has passed since t = 0 s [s].*

2.2. Ion-exchange chromatography method

In the scope of this research is also the automatization and standardization of the ion-exchange chromatography method for scandium separation [29]. Previous work has focused on the method evaluation and optimization; however, more work was required on the parameter standardization and ease of use and is reported in this document in this section.

2.2.1. Types of columns used and other materials

Two types of column diameters – 3 and 5 mm were tested. Unfortunately, due to ICP-MS device malfunction no clear results from ^{45}Sc tests using ion-exchange chromatography can be shown at the time of the preparation of this document (to be measured by mid-September 2023, at the University of Latvia).

The materials/ equipment used was as follows:

1. Diba Omnifit Microbore Benchmark chromatography column (100 mm, inner Ø 3 mm), EW-11941-08
2. Diba Omnifit EZ chromatography column with 1 adjustable and 1 fixed endpiece (100 mm, inner Ø 5 mm), EW-11942-76
3. ICP-MS standard solutions (1000 mg/L), Alpha Aesar, AAS standard, Specpure, in 5 % HNO_3;
4. Hydrochloric acid, 37%, ACS reagent grade, Sigma Aldrich
5. Nitric acid 70%, ACS reagent grade, Sigma Aldrich;
6. Laboratory stands with clamps;
7. Peristaltic pump for column Ismatec ISM-834C, 1-100 μL/s;
8. Peristaltic pumps for sample and eluent transport Masterflex 73160-25, 20 rpm, 12 V, 0.5 A;
9. Masterflex pump power supply Ansmann APS600, 735 0731;
10. Deionized water (0.055 μS/cm);
11. Analytical balance Pioneer, 0.0000 – 210.0000 g, ± 0.0001 g;
12. DGA resin – branched, Eichrom Industries, size 50 – 100 μm, bulk;
13. Glass sample vial, 20 mL, PerkinElmer;
14. Fume hood;
15. Automatic pipettes (10.0 ± 0.2 μL, 1000 ± 20 μL, 5000 ± 100 μL, and 10.00 ± 0.02 mL) and tips;
16. Volumetric flasks, 10.00 ± 0.02 mL; 25.00 ± 0.04 mL; 50.00 ± 0.06 mL; 100.0 ± 0.1 mL;

17. Ultrasonic bath Bandelin Sonorex, 160 – 640 W;
18. Radiameter ThermoScientific FH 40G-L10 (10 nSv/h – 100 mSv/h; 30 keV – 4.4 MeV);
19. Gamma spectrometer Canberra Cryo-Pulse 5 plus GX4020, bias voltage 3.5 kV, Apex gamma software, detection limit for ^{47}Sc: as low as 100 Bq, depending on measurement time.
20. X-ray fluorescence detector (XRF) ThermoScientific Niton XL3t, precious metal library;

The resin mass used was ~0.10 g for 3 mm column achieving bed hight of 3 cm and 0.18 g for 5 mm inner diameter column resulting in a bed hight of 3.2 cm.

2.2.2. Column fitting testing and treatment

The 3 mm inner diameter column fittings feature a SS316 frit disc that may be prone to corrosion under acidic environment. Due to the nature of nitric acid, after treatment with 8 M HNO_3 for 24 h, a passivation layer is to be achieved that prevents further oxidation. [32] However, hydrochloric acid attacks SS316 regardless of the passivation layer, the reaction rate depending on the concentration.

Tests using 8 M HNO_3 were conducted as follows:

1. Holding in 5 mL of 8 M HNO_3 for 24 h;
2. Rinsing with deionized water;
3. Holding again in 5 mL of 8 M HNO_3 for 24 h;
4. Rinsing with deionized water;
5. Holding in 5 mL deionized water for 24 h;
6. Sample preparation for ICP-MS.

A schematic representation of the analysis is shown in Fig. 7.

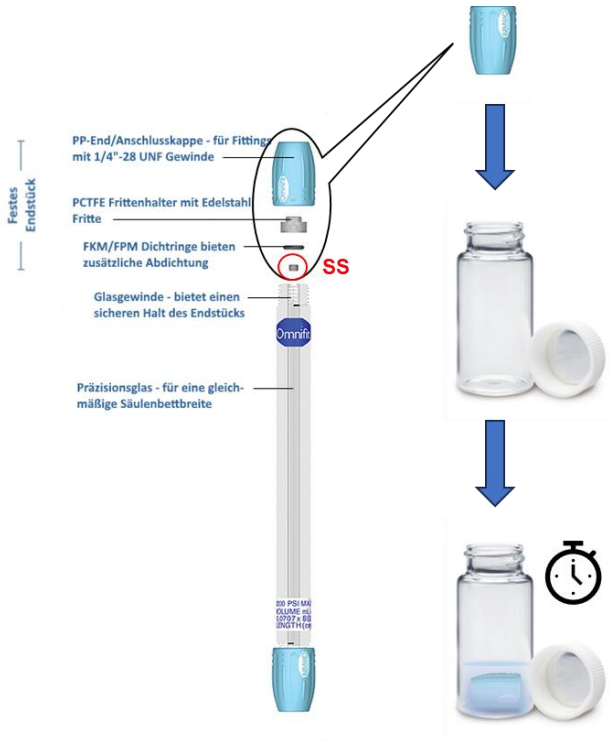

Fig. 7. **Diba Omnifit Benchmark Microbore Chromatography column (3 mm inner diameter) scoping test procedure**

The manufacturer provides information that the fitting SS316 discs with 2 μm pore size are resistant to HCl with concentration < 10 % and < 50 % HNO_3. [33]

Experiments in the future should also be conducted using 0.1 M HCl to verify the company's claims of corrosion resistance for HCl < 10 %.

2.2.3. Column setup automatization – experimental validation

A semi-automated setup was created to evaluate the potential for further automation and the possible limitations. The setup shown in Fig. 8. was used for both stable and radioactive Sc separation (2^{nd} separation only).

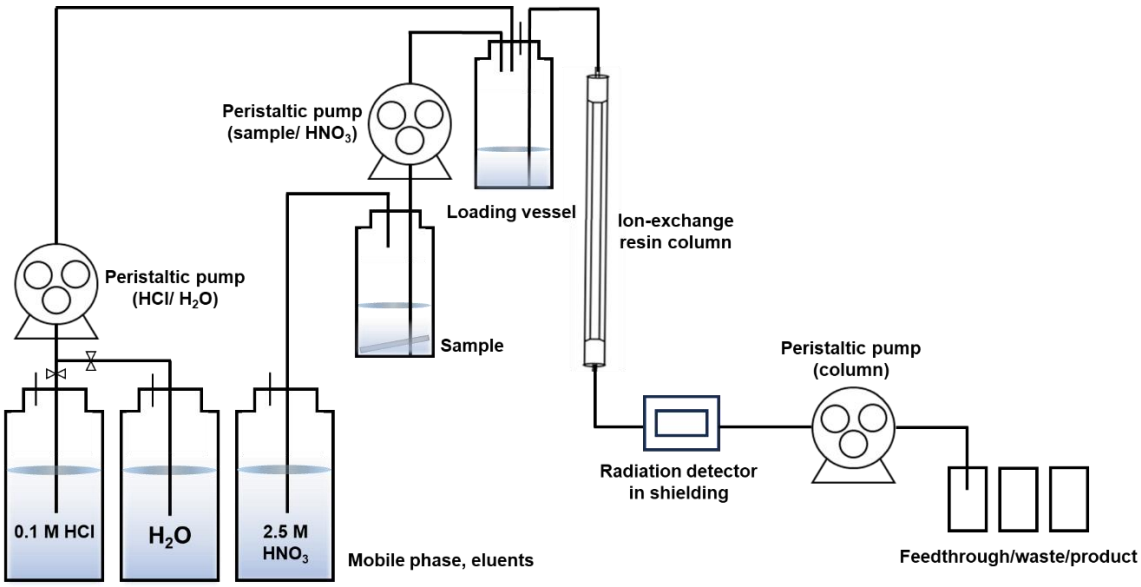

Fig. 8. **Semi-automated Sc ion-exchange chromatography separation setup**

A photograph of the complete setup can be seen in Fig. 9.

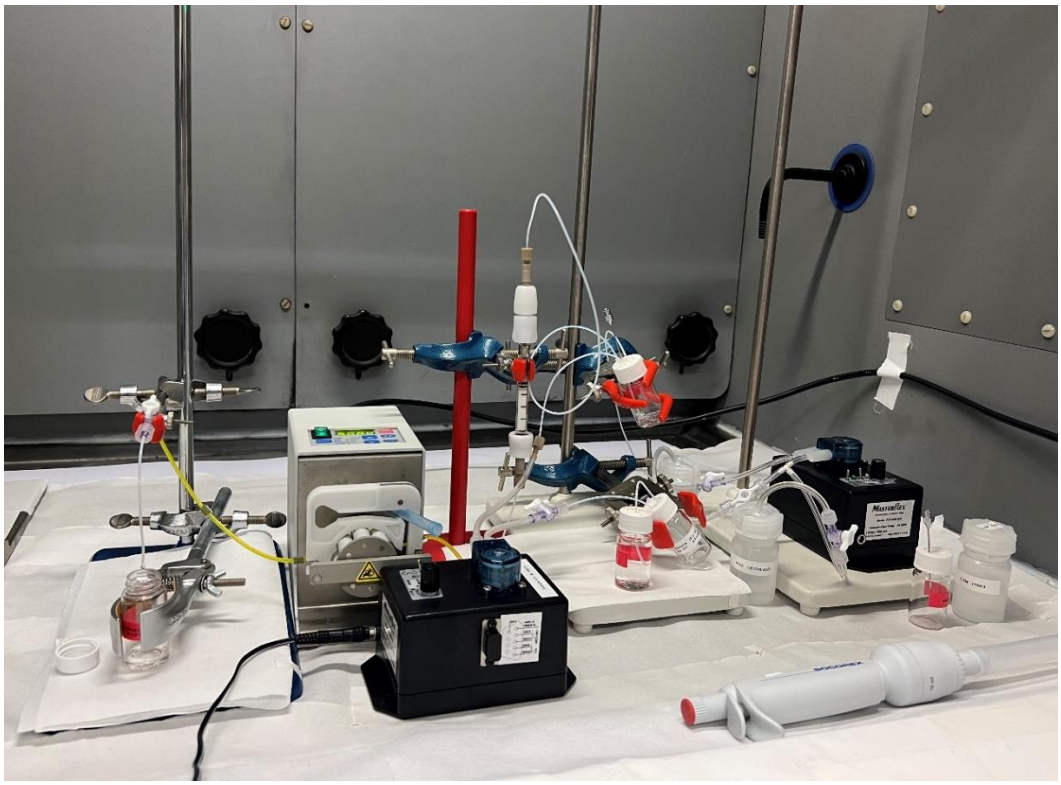

Fig. 9. **Semi-automated Sc ion-exchange chromatography separation setup photograph**

The main advantages of this setup are:

1. Sample can be introduced while in shielding (important for cases of high activity) and the whole system can be set up to be controlled remotely (not done for the experiments carried out).
2. The only interaction with radioactive material is the collection and capping of radioactive product fraction (can be further automated using a carousel for fraction collection).
3. No air can leak into the column – there is always solvent in the loading vessel, all capillaries are submerged (for radiation protection purposes - can be replaced in case of contamination).
4. The mobile phase and eluent can be easily transferred to the loading vessel and thus the column using separate peristaltic pumps with pre-set flow rates.
5. A Geiger-Muller counter can be used to trace and monitor radioactive inventory movement in the system. It also allows for chromatographic parameter estimation (e.g., resolution).
6. The flow rate can be easily adjusted by monitoring the output of the liquid (one droplet is equal to ~ 0.03 mL), therefore, counting the number of droplets in a specified time allows the calculation of the flow rate more precisely than weighing the collection vials (due to the density of the liquid being >> 1 g/ cm^3).

2.2.4. Ion-exchange chromatography resin performance evaluation

To evaluate the DGA resin performance the ion-exchange capacity (IEC) should be considered. It is the measure of how much ions (like Sc^{3+}) can be held by a certain mass of the resin. In order to calculate the IEC, the column must be oversaturated with Sc so that passing new Sc^{3+} ions they pass through freely. Knowing the amount of Sc^{3+} ions loaded in/ through the column, ICP-MS can be used to determine the amount of ions that were not adsorbed and thus calculate the IEC as stated in the equation below (Equation 16):

$$IEC = \frac{(n_{Sc^{3+}{}_{loaded}} - n_{Sc^{3+}{}_{passed}}) \cdot 10^3}{m_{resin}} \quad (16)$$

where *IEC – ion exchange capacity [mmol/g],* $n_{Sc^{3+}{}_{loaded}}$ *– amount of* Sc^{3+} *ions fed into the column [mol],* $n_{Sc^{3+}{}_{passed}}$ *– amount of* Sc^{3+} *ions that have passed through the column (determined by ICP-MS) [mol],* m_{resin} *– mass of the resin loaded into the column [g].*

2.2.5. ^{45}Sc separation using ion-exchange chromatography (stable tests)

The overall setup integrity was tested using ^{45}Sc ICP-MS standards. The elemental compositions were the same as the ones for electrochemical separation. Both Diba Omnifit Microbore Benchmark 3 mm and Diba Omnifit EZ adjustable dead-volume 5 mm inner diameter columns were used. Samples are named based on the column type used and the experiment number (*YY* IE *X*, where *YY* – column type, IE – ion-exchange, and X – experiment number).

Prior to the experiment, DGA resin has to be soaked in 2.5 M HNO_3 for a period of ~ 24 h (insert reference why).

The general procedure is as follows:

1. Load column with resin (slurry of DGA in 2.5 M HMO_3);
    a. Flush column with ~10 mL 2.5 M HNO_3 – 1 waste vial;
2. Dissolve the foil Al, Zn or NaCl coating in 3 mL 2.5 M HNO_3 (in case of ICP-MS standards – the addition of analyte into the sample vial);
    a. Load in the column, collect Feedthrough (*YY* **FE** *X*);
3. Wash column with 5 mL 2.5 M HNO_3;
    a. Continue collecting in Feedthrough vial;
4. Elute with 6-10 mL 0.1 M HCl;
    a. Collect in Product vial (*YY* **P** X);
5. Wash the resin with 10 mL H_2O;
    a. Collect wash vial (*YY* **WH_2O** *X*);
6. Treat the resin with 2.5 M HNO_3 (optional regeneration step) or dispose of as organic material non-halogen waste, flush system with 2.5 M HNO_3.

The samples are shown in Table No. 3.

Table No. 3. **^{45}Sc ion-exchange chromatography sample identification and parameters**

Sample name	Element	Mass concentration (theoretical; before electrolysis), mg/L	Ratio to Sc	Additional info
D3IE1	Na	100000	$5.0 \cdot 10^6$	V target
	Sc	0.020	1.0	
	Al	0.40	20	
	Ti	0.40	20	
	Rb	0.40	20	
	V	40	$2.0 \cdot 10^3$	
D3IE2	Na	100000	$5.0 \cdot 10^6$	TiC target
	Sc	2.8	1.0	
	Al	0.40	20	
	Ti	0.40	20	
	Rb	0.030	20	
	V	0.030	$2.0 \cdot 10^3$	
D5IE1	Na	100000	$5.0 \cdot 10^6$	V target
	Sc	0.020	1.0	
	Al	0.40	20	
	Ti	0.40	20	
	Rb	0.40	20	
	V	40	$2.0 \cdot 10^3$	
D5IE2	Na	100000	$5.0 \cdot 10^6$	TiC target
	Sc	2.8	1.0	
	Al	0.40	20	
	Ti	0.40	20	
	Rb	0.030	20	
	V	0.030	$2.0 \cdot 10^3$	

At the time of this report no ICP-MS measurements could be performed due to device malfunction.

2.2.6. ^{47}Sc separation using ion-exchange chromatography (radioactive tests)

The ion-exchange procedure for radioactive scandium isotopes (tested for ^{47}Sc) is identical to the ^{45}Sc procedure, however, a foil is present in the case of ^{47}Sc

requiring small modifications to the procedure (please see in detail below, refer to Fig. 8 for the setup and component identification):

1. Before the procedure, DGA resin is soaked in 2.5 M HNO_3 for 24 h. The gamma spectrometry measurement for the sample should be known at this stage;
2. The resin slurry is loaded into the column, noting the packing and height of resin (automatically by the use of a peristaltic pump for 3 mm inner diameter column, flow rate maximum 1 mL/min to produce even packing; manually for 5 mm inner diameter column, flow rate as high as 5 mL/min);
3. System connected as per Fig. 8. and 9.
4. The column is flushed with ~10 mL 2.5 M HNO_3 by pouring 20 mL into the 2.5 M HNO_3 vessel (right before the sample) and switching on the sample/ 2.5 M HNO_3 peristaltic pump at ~ 1 mL/ min (20 rpm);
5. When > 1 mL has accumulated in the loading vessel, the column peristaltic pump is turned on, flow rate set to 5.00 μL/s which corresponds to ~0.40 mL/ min;
6. The waste HNO_3 that was used to condition the column is collected in a vial labeled YY **WHNO$_3$** *X*;
7. When 10 mL are left in the 20 mL HNO_3 reservoir next to the sample position, 3 mL of 2.5 M HNO_3 is added to the sample vial – NaCl coated Al foil or Zn/ Al coated Au foil is switched for the previous vial in the sample position;
8. The foil is placed so, that fresh HNO_3 drips directly onto the surface ensuring quantitative transfer;
9. Once this step is initiated, feedthrough (*YY* **FE** *X*) is collected until all the liquid in HNO_3, and sample reservoir has been transferred to the loading vessel. Then the sample/ HNO_3 peristaltic pump is turned off;
    a. Dose rate is measured in the column and feedthrough vial *YY* **FE** *X;*
10. When the liquid level in the loading vessel drops to ~ 1 mL, HCl/ H_2O peristaltic pump is switched on to introduce 0.1 M HCl to the loading vessel. The flow rate is set to 0.8 mL/min. Once HCl has entered the loading vessel, the feedthrough (*YY* **FE** *X*) fraction is changer for the product (^{47}Sc) collection (*YY* **P** *X*);
    a. Elution profile can be obtained placing a gamma detector in front of the *YY* **P** *X* vial and registering as a function of time/ flow rate. This also allows to monitor the elution process – gives information of the radioactive inventory location;

11. The column peristaltic pump flow rate can be increased up to 10 μL/s, corresponding to 0.6 mL/min;
12. Once 5 - 10 mL are collected in *YY* **P** X vial, the HCl/ H_2O peristaltic pump is turned off, and using valves, liquid is rerouted, and the peristaltic pump is switched back on to provide H_2O to the loading vessel and thus the column in order to wash the column;
13. As soon as the previous step is carried out, the *YY* **P** X vial is switched to *YY* **WH_2O** *X* and 10 – 15 mL are collected;
14. The activity is measured in the loading vessel, column, and wash vial *YY* **WH_2O** *X*. If no activity can be seen in the loading vessel or column, it can be assumed that the system is successfully flushed – cleaned to be disassembled (if needed);
15. Gamma spectrometry measurements are performed for all the collected vials as well as the now assumed empty (of radioactive substances) foil;
16. Should the resin be reused, treatment with 2.5 M HNO_3 (optional regeneration step) can be carried out or it can be disposed according to pertinent regulations.

The ion-exchange ^{47}Sc recoverability (Equation 17) can be evaluated by relating the retrieved (eluted) ^{47}Sc activity to the initial ^{47}Sc activity on the Zn/ Al coated Au or NaCl coated Al foil (the activity is time-corrected):

$$\varphi = \frac{A_{elute}}{A_{foil}} \cdot 100 \tag{17}$$

where φ *– ion-exchange separation recoverability of* ^{47}Sc *(yield) [%],* A_{foil} *– activity on the foil before radiochemical procedure [Bq],* A_{elute} *– activity in the eluted liquid [Bq].*

Two separations with ^{47}Sc were carried out (25/08/2023 and 04/09/2023 respectively) using a basic ion-exchange chromatography setup (see Fig 10) for the first separation and the semi-automated setup for the second (Fig. 8 and 9).

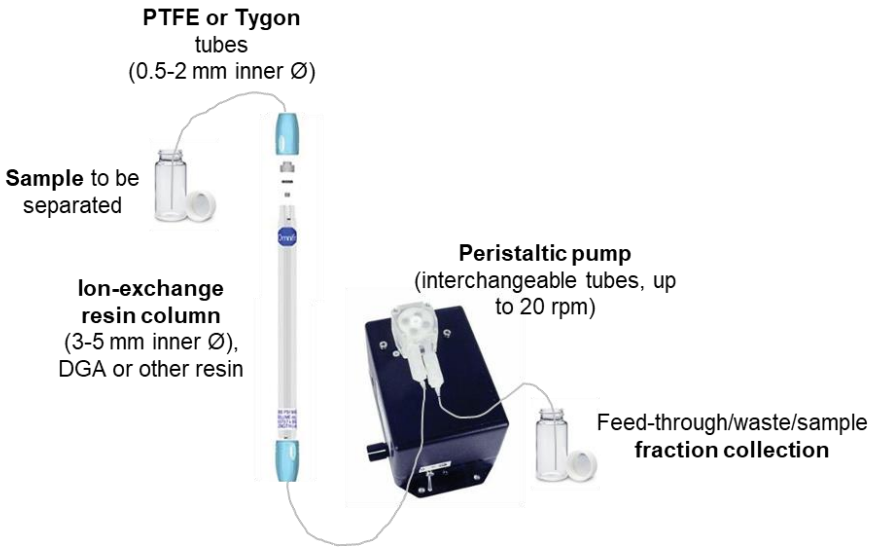

Fig. 10. **Basic pump-assisted ion-exchange chromatography setup Diba Omnifit Benchmark Microbore Chromatography column (3 mm inner diameter)**

First separation featured 3 mm Diba Omnifit Benchmark Microbore column (in Fig. 10.), whereas the 2nd separation featured a 5 mm adjustable dead-volume Diba Omnifit EZ column (seen in Fig. 9.).

2.2.7. Column setup automatization – proposed further automatization

The setup used in the framework of the study reported in this document can be further automatized to fully evade human physical interaction with the system.

A proposed system is shown in Fig. 11.

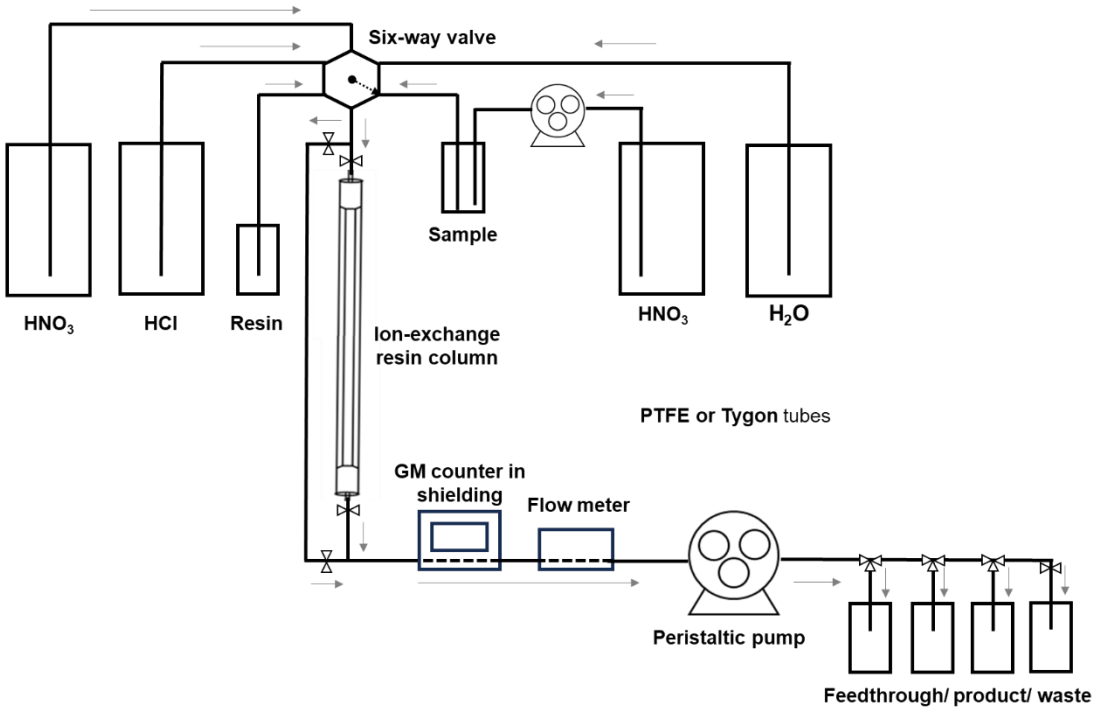

Fig. 11. **Proposed fully automated ion-exchange chromatography setup**

The main difference between the setup used experimentally and this proposed system is the use of a six-way valve and a column bypass tube. The other main difference is the automatic control of the valves – using digital data transmission to change the position of the valve. Furthermore, since the flow rate is measured, the pump speed can be varied automatically (current controller responding to the change of flow rate measurement).

The collection vials can also be placed inside a sample collection carousel that changes position depending on a pre-set volume or time. Another benefit of this setup is the automatic loading of resin.

3. RESULTS

The results are shown in accordance with the experimental section. The performance of both electrochemical and ion-exchange methods is compared and evaluated.

3.1. Electrochemical method

The electrochemical separation of contaminant ions has been evaluated and the best conditions and parameters have been described.

3.1.1. Electrochemical method parameter optimization

Multiple parameters appear to affect the possible current values for aqueous metal ion solution electrolysis.

Data acquired (in the case of Fig. 12 – current by Keithly 2000 multimeter, temperature by hand from a glass thermometer) is shown in Fig. 12 indicating both current and temperature.

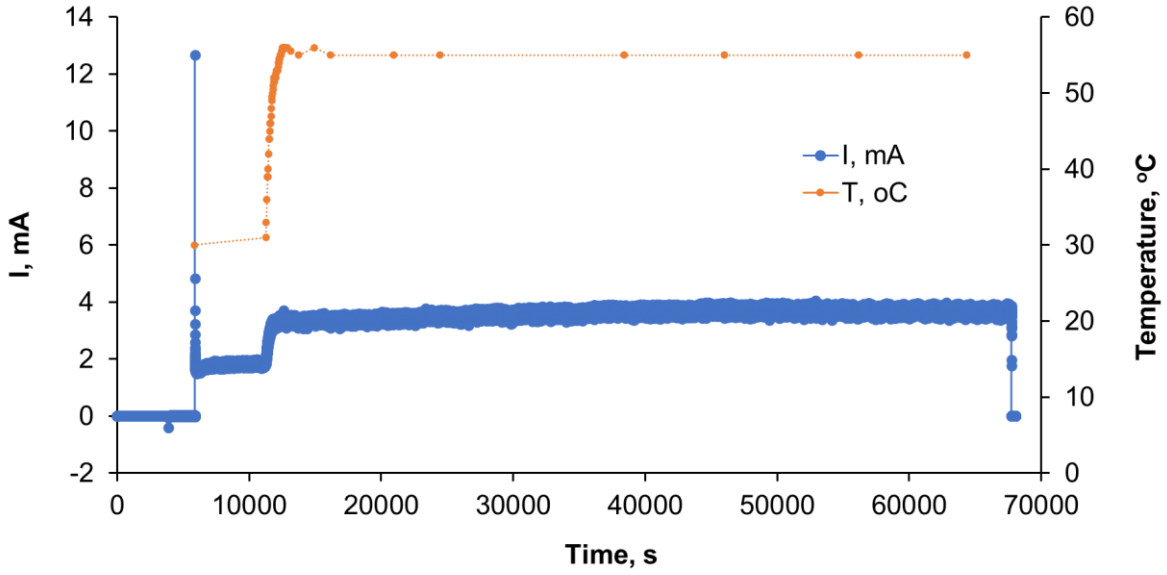

Fig. 12. **Current data depending on the temperature of the sample (ES5)**

Data in Fig. 12 shows the impact of temperature (and thus – ion mobility) on current. An increase of 25 °C yields in the increase of current by 2 mA. The effect of temperature here is so noticeable due to the low ionic strength (0.008 M). [30] In cases where the ionic strength was >> 1 M almost no effect of temperature increase correlating to current increase was noticed. Temperatures above 55 °C were not used due to the rapid evaporation of water from solution [18].

The impact of the ionic strength was also shown by adding electrolyte during electrolysis (Fig. 13).

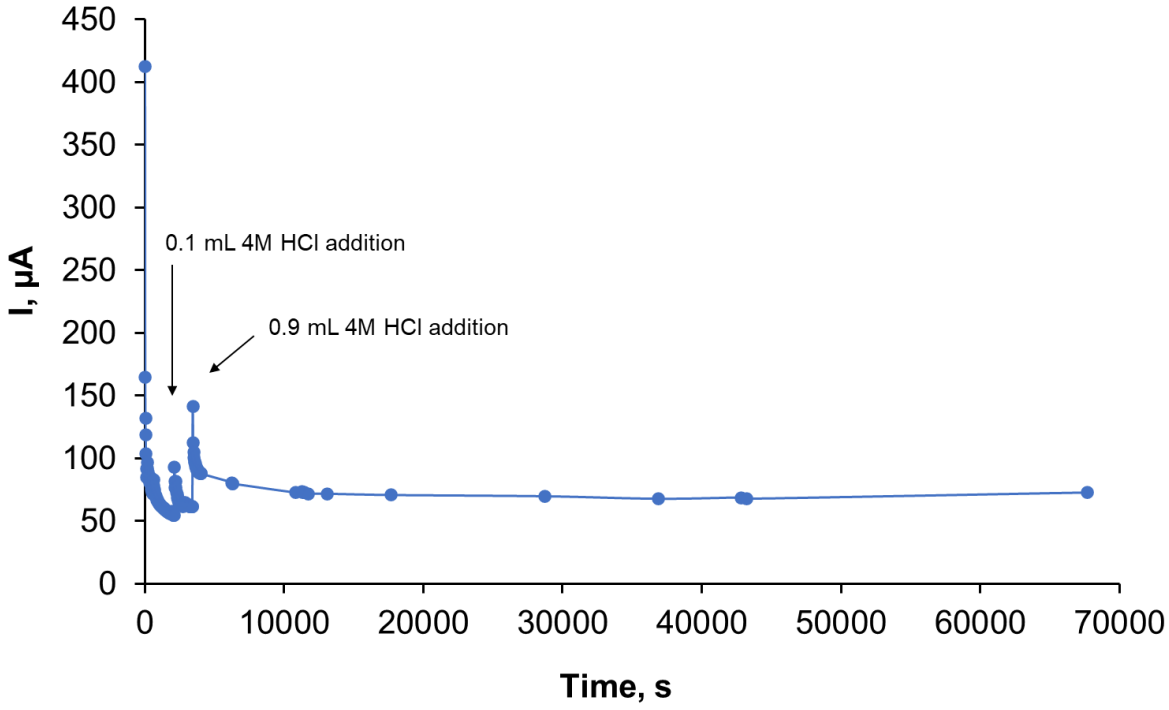

Fig. 13. **Current data depending on the addition of 4 M HCl (increase of ionic strength)**

The ionic strength of the solution impacts the current, which could be both due to the undesirable hydrogen evolution reaction on the cathode as well as the increased migration of metal ions (which need to be deposited) due to large ionic strength. [30]

Due to electrode polarization (use of direct current) sample stirring is necessary – generally the higher the stirring, the larger the current due to more efficient ion migration.

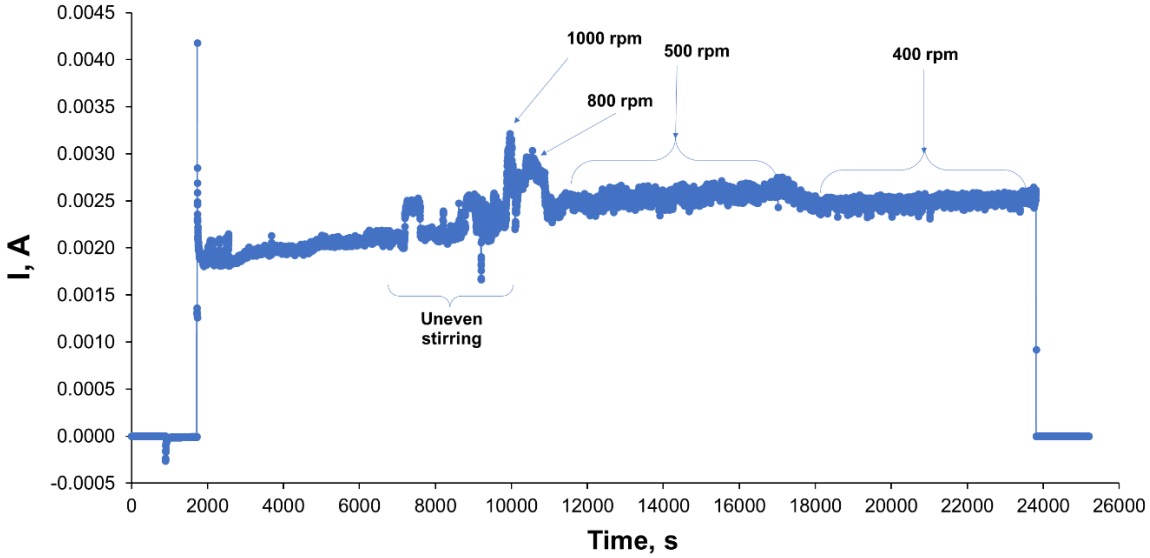

Fig. 14. **Current values depending on the stirring rate (rpm) of the solution**

From Fig. 14 it can be seen that stable current values were achieved by 400 and 500 rpm (for the stirrbar – agitator). However, it was found that 600 rpm also produces stable current (as in Fig. 12) and does not splash out any liquid as 1000 rpm might in cases of uneven magnetic fields.

Further experiments and calculations are necessary to also evaluate the current densities and electrode material/ size/ shape impact.

3.1.2. ^{45}Sc electrochemical separation (stable) tests

The method was reviewed and studied mostly by the use of stable ^{45}Sc ICP-MS standards.

Current data is shown for ES1-ES3 samples in Fig. 15.

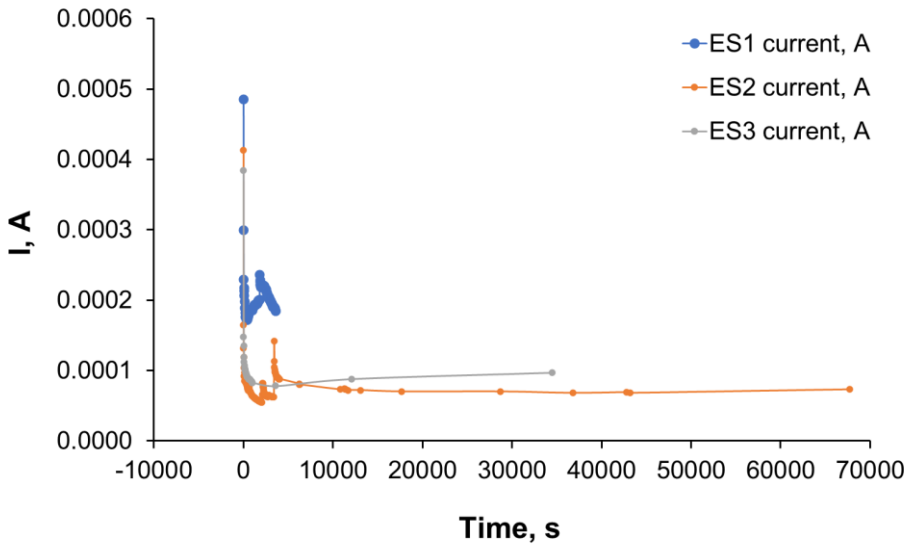

Fig. 15. **Current data for samples ES1-ES3**

A summary of samples that were analyzed (samples after ES3 as listed in the Experimental section have not been analyzed at the time of this report due to ICP-MS device malfunction) is shown in Table No. 4.

Table No. 4. **Samples ES1-ES3 showing ICP-MS results for ion concentrations**

Sample	Element	Theoretical mass concentration before electrolysis, mg/L	Actual mass concentration before electrolysis (ICP-MS), mg/L	Actual mass concentration after electrolysis (ICP-MS), mg/L
ES1	Al	40	52.8	47.3
	Sc	2.4	2.70	2.49
	Ti	0.030	0.162	0.0301
	V	0.030	0.0387	0.0361
	Ca	0.030	0.938	0.446
ES2	Al	40	52.8	31.0
	Sc	2.4	2.70	1.73
	Ti	0.030	0.162	0.0213
	V	0.030	0.0387	0.0229
	Ca	0.030	0.938	0.287
ES3	Ti	330	>0.5	>0.5
	Al	24	23.1	21.8
	Sc	0.00033	<0.001	<0.001
	Ca	0.00026	4.26	4.20

The ICP-MS results for samples ES1 and ES2 are summarized in Fig. 16.

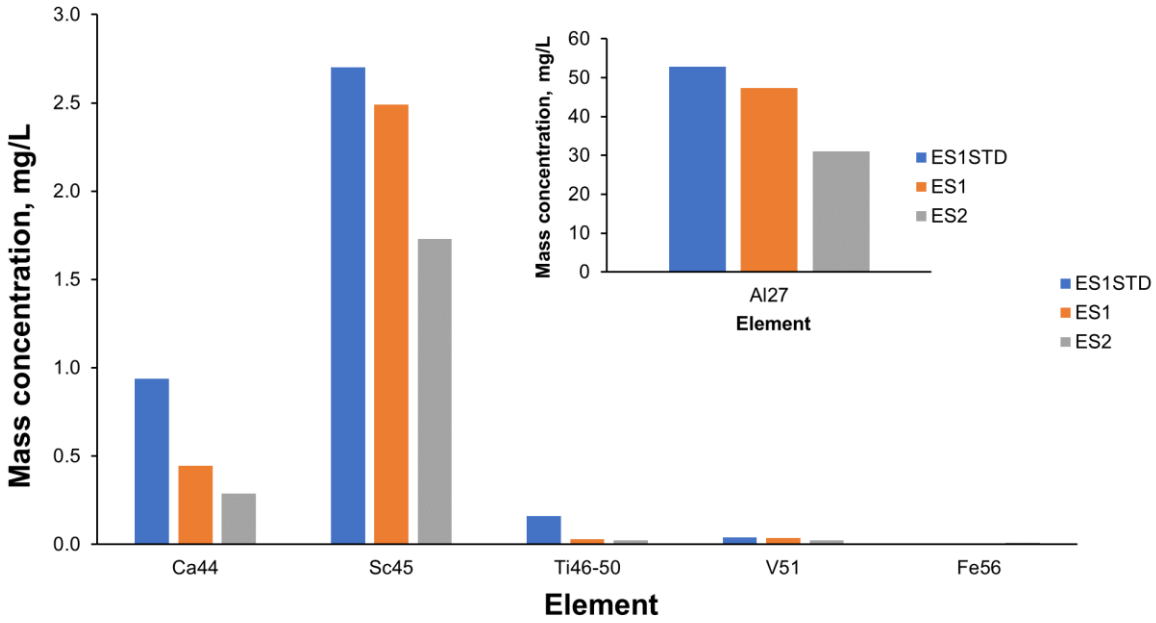

Fig. 16. **ICP-MS data showing ES1-ES2 elemental composition (blue – initial, orange – ES1, gray – ES2)**

The results show inconsistencies with theoretical and practical observations – an element such as Ca cannot deposit during electrolysis due to the low redox potential and high activity (reacts with water). Ca deposition in solution was not possible due to the pH being < 0.1. The most reasonable explanation would be the lowering of concentration due to accidental dilution of the samples. However, this would also mean that the rest of the ions should have decreased in concentration by the same ratio. However, Ca has decreased by 52 %, whereas Sc (also should not have deposited under the experimental conditions) has decreased only by 8 %. This disproves the accidental dilution possibility.

More research would be needed to investigate this occurrence such as repetitions of the same experiments in the same conditions and using different ICP-MS devices to compare the results and estimate the sources of errors.

Due to the errors in Ca determination these results can be regarded as somewhat incorrect and should not be used for method evaluation even though a decrease in Ti, V and Al ions is noticeable.

For sample ES3, the results are shown in Fig. 17.

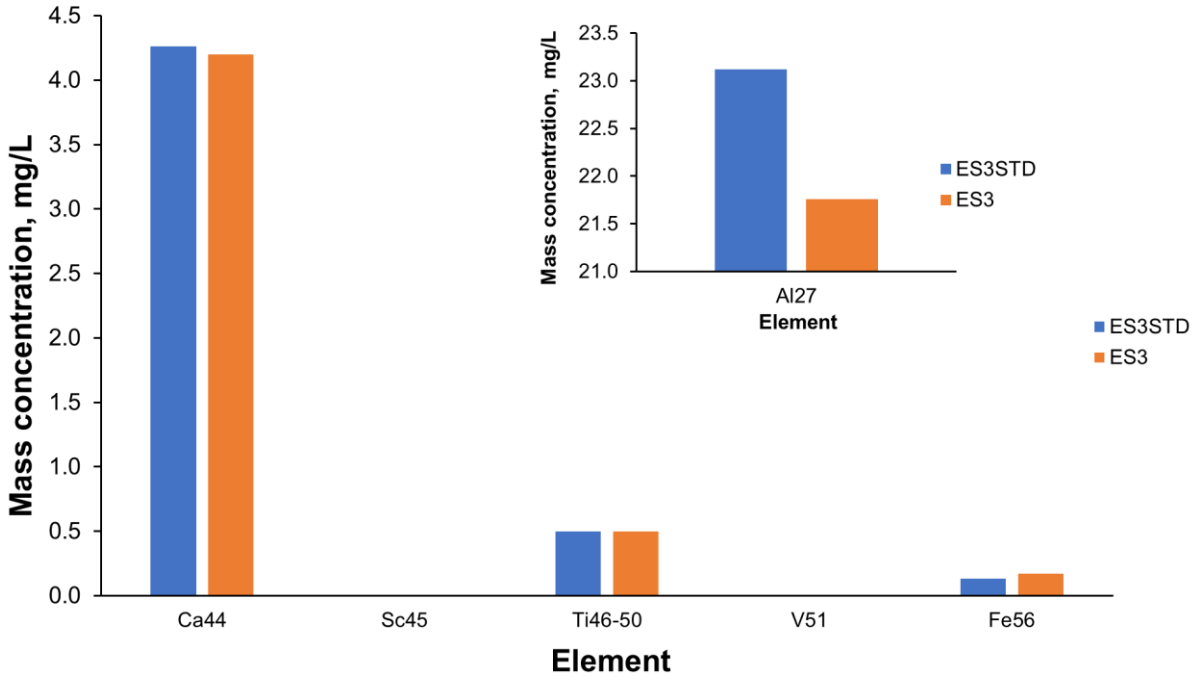

Fig. 17. **ICP-MS data on the ES3 elemental composition (blue – initial, orange – ES3)**

For ES3, the concentration of Sc is < LoD and for Ti is > maximum measurable value. However, the amount of Ca seems to be the same (4.26 mg/L in initial standard and 4.20 mg/L for the electrolyzed solution of the standard), therefore, these results can be interpreted as valid.

A difference can be seen for aluminum – the concentration has decreased by 6 %. Comparing to the theoretical amount deposited by electrolysis to the ICP-MS results (Equations 10-14) gives an **efficiency of 41 ± 2 %.** Such efficiency is very good due to the low (below H_2O) redox potential. [13,34] However, more measurement calculations are needed (not possible at the time of this report due to ICP-MS malfunction) to interpret parameter like current density, ion activity and temperature impact on the efficiency.

In order to increase the efficiency a non-aqueous solvent should be used. Should a non-aqueous solvent be used efficiency up to 100% can be expected both for contaminant removal and Sc collection directly on an electrode. [12]

3.1.3. ^{47}Sc electrochemical separation (radioactive) tests

Using ^{47}Sc collected on a NaCl coated Al foil (15/08/2023, as per [7]) an electrochemical separation test was carried out. The results acquired with gamma spectroscopy (carried out by Charlotte Duchemin) and (activity corrected for 25/08/2023) are shown in Table No. 5

Table No. 5. **Gamma spectrometry results for the first ^{47}Sc separation procedure**

Sample name	Measurement time, s	**Activity, Bq**	Uncertainty, %
^{47}Sc on NaCl coated Al foil	903.4	**8698 ± 965**	11.13
ERSC2	6017.5	**x**	x
ERSC1	5415.6	**x**	x
^{47}Sc liquid fraction	1805.4	**6516 ± 820**	12.58
Empty Al foil	10831.3	**323 ± 109**	33.68
ERSA1 and ERSA2	10029.2	**692 ± 234**	33.79
Diba Omnifit Benchmark column 3 mm diameter	10832.6	**x**	x

The initial activity was 8698 ± 965 Bq of which 3.7 % was left on the Al foil (possibly – implanted in Al) and a further 8.0 % was left on the anodes used in electrolysis. This is due to the porosity of electrodes – not all the solution could be rinsed out leaving some ^{47}Sc behind. This, however, was the reason for investigating electrode platinum plating described in the next chapter.

The acquired data does not give any indication on how successful the electrochemical contaminant separation was, however, it proved that Sc cannot be deposited on an electrode in aqueous electrolysis. Therefore, steps 15-19 should be excluded from the experimental procedure . For the ICP-MS analysis of the obtained fractions, various amount of time has to pass, up to 2 months since 25/08/2023 to consider the samples non-radioactive.

3.1.4. Electrode surface platinum plating

Since the issue of ^{47}Sc losses in the porous electrodes was noticed in the 25/08/2023 radiochemical separation (see chapter 3.1.3), a solid Pt layer was introduced on a pair of electrodes (C4(-) and (A4(+)).

The amount of $PtCl_2$ used in each experiment varied from 0.02 g (1st Pt coating experiment) to 0.05 g for the 2nd platinum coating experiment.

The surface of the electrodes was analyzed with XRF (X-ray fluorescence spectroscopy). Firstly, the acquired background values (identical within the measurement uncertainty for anode and cathode) were measured and are displayed together with the elemental composition of platinum covered electrode acquired using precious metal setting in Table No. 6.

Table No. 6. **Graphite electrode platinum covering XRF analysis results**

Electrode	Element	Percentage of total elements, %
A1(+) and C1(-), non-platinated	Ti	70.5 ± 0.6
	Cr	21.9 ± 0.6
	Mn	3.34 ± 0.11
	Ni	2.02 ± 0.07
	Ag	1.39 ± 0.05
	Co, Au, Cu, Zn	< 0.30 ± 0.02
C4(-), Pt coating experiment No. 1	Ti	68.7 ± 0.5
	Cr	15.6 ± 0.4
	Pt	**10.2 ± 0.2**
	Mn	2.39 ± 0.07
	Ni	1.30 ± 0.04
	Ag	1.26 ± 0.04
	Co, Au, Cu	< 0.200 ± 0.02
A4(+), Pt coating experiment No. 2	Ti	59.6 ± 0.7
	Pt	**27.8 ± 0.5**
	Cr	9.2 ± 0.3
	Mn	1.41 ± 0.06
	Ag	1.04 ± 0.05
	Ni, Ir, Co, Zn	< 1.00 ± 0.06

The large titanium content can most likely be attributed to carbon. The explanation is that carbon has a very low X-ray fluorescence yield [35] K absorption edge for carbon is 283 eV [35], accounting for the large gap between the energy provided between the K edge and XRF gun produced X-rays. Ti has gamma XRF lines at 4.51 and 4.93 keV. [36]

Any additional metals like Cr, Mn and Ag do not pose an issue as they are either trapped behind the Pt covering or were afterwards dissolved by treatment with 2.5 M HCl for 5 h.

This method can also be used to separate platinum isotopes from other elements for medical applications.

3.2. Ion-exchange chromatography method

The results for ion-exchange chromatography setups and columns tested are summarized in this section.

3.2.1. Column fitting testing and treatment

The 3 mm inner diameter column fittings with stainless steel frit discs were tested using HNO_3. The results from ICP-MS are shown in Table No. 7

Table No. 7. **Diba Omnifit Microbore Benchmark chromatography column (3 mm inner diameter) fitting testing and treatment results**

Procedure step	Ion	Ion concentration, mg/L
First hold in 5 mL 8 M HNO_3 for 24 h	Al^{3+}	2.98
	Ti^{3+}	0.0735
	Fe^{3+}	**1.29**
Second hold in 5 mL 8 M HNO_3 for 24 h	Al^{3+}	1.44
	Ti^{3+}	0.0111
	Fe^{3+}	**0.139**
Hold in 5 mL H_2O for 24 h	Al^{3+}	< 0.5
	Ti^{3+}	0.0022
	Fe^{3+}	**< 0.001**

As can be seen from Table No. 7, nitric acid with 8 M concentration does appear to form a protective layer: the amount of iron present in the second hold is ~ 10 times less than the first. Washing with deionized H_2O shows no corrosion products are remaining in the fitting.

In Sc separation procedure, 2.5 M HNO_3 is used (> 10 % concentration), therefore, due to this pre-treatment procedure no interaction with the frit discs is to

be expected. For elution purposes 0.1 M HCl is used which is << 10 % concentration corresponding to manufacturer's chemical compatibility evaluation [33].

Diba Omnifit columns (3 and 5 mm inner Ø) were tested, however, due to ICP-MS device malfunction the results will be available after measurement at the University of Latvia in mid-September 2023.

3.2.2. ^{45}Sc ion-exchange separation (stable) tests

Tests of both Diba Omnifit Microbore Benchmark 3 mm and Diba Omnifit EZ 5 mm inner diameter columns were carried out in order to verify the setup – acceptable flow rates (0.3-0.9 mL/min) and to check for possible leakages.

It must be noted that the 5 mm column features an adjustable frit disc plunger to decrease the dead volume.

No leakages were discovered, and fractions were successfully collected, however, no results can be shown at the time of this report due to ICP-MS malfunction.

3.2.3. ^{47}Sc ion-exchange separation (radioactive) tests

Two ^{47}Sc radiochemical separations were carried out – on the 25/08/2023 and 04/09/2023.

The first separation (25th August 2023) was done in combination with electrochemical separation (using setup shown in Fig. 6 and 10) and the time-corrected radioactivity values are shown in Table No. 5.

The column used was Diba Omnifit Benchmark Microbore with 3 mm inner diameter, 3 cm resin bed hight. Since some ^{47}Sc was lost in the electrochemical separation due to the porosity of the electrodes, this part (8.0 %) is disregarded in the efficiency calculation of ion-exchange chromatography.

Since the total radioactivity initially produced was 8698 ± 965 Bq and 8.0 % was lost due to the electrodes, the initial radioactivity is corrected to 8006 ± 880 Bq. The radioactivity separated by ion-exchange chromatography is 6516 ± 820 Bq and calculating the efficiency of **^{47}Sc radiochemical recoverability gives 81.4 ± 1.2 %.**

Due to connection difficulties regarding the setup the overall process took **3.5 hours,** and the maximum flow rate was 0.34 mL/ min.

The results are summarized in Fig. 18.

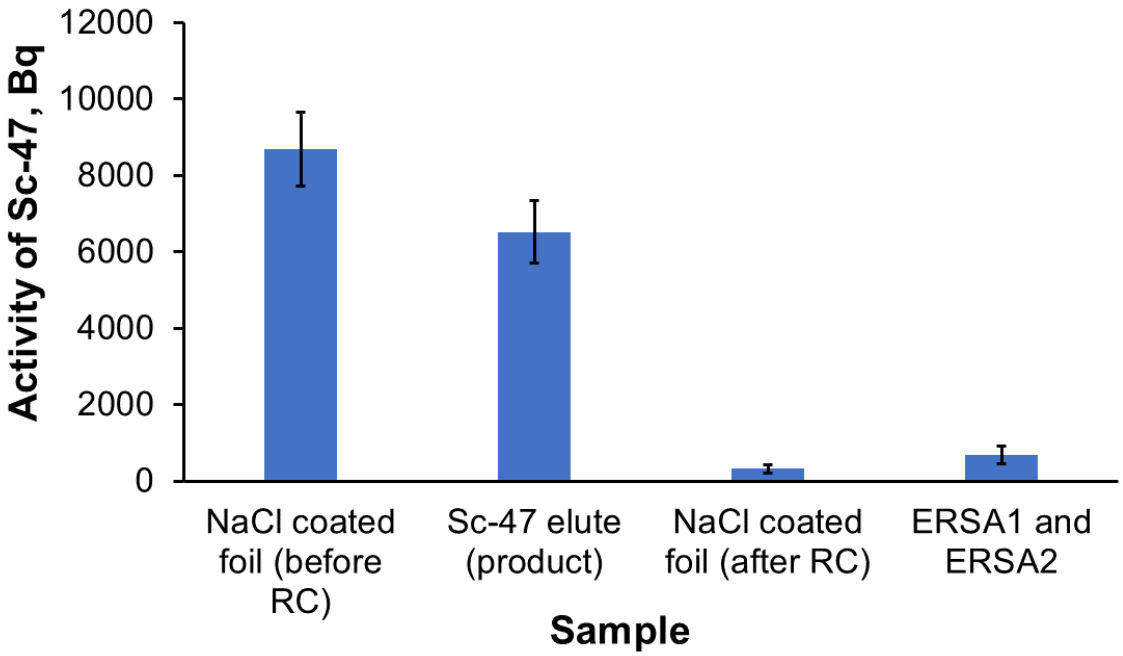

Fig. 18. **Gamma spectrometry results for the 1st ^{47}Sc separation (combination of electrochemical and ion-exchange chromatography, activity half-life corrected**

It must be noted that since no activity is left in the column, feedthrough, or H_2O fractions it can be assumed that the **actual recoverability is 95.03 %** (accounting for **4.96 % left in the Al foil** most probably due to implantation of ^{47}Sc in bulk which was not attacked by the 2.5 M HNO_3).

Should the leftover material in the foil be disregarded, the **^{47}Sc radiochemical recoverability** is **~ 99.9 %.** However, ICP-MS results are needed to evaluate the separation efficiency from contaminant ions.

For the 2nd radiochemical separation only the ion-exchange method was tested using a column of 5 mm inner diameter with resin bed hight 3.2 cm. The separation was carried out using a semi-automated setup (Fig. 8 and 9).

The gamma spectroscopy results are shown in Table No. 8.

Table No. 8. **Gamma spectrometry results for ^{47}Sc 2nd separation (only ion-exchange chromatography), activity half-life corrected**

Sample name	Measurement time, s	Activity, Bq	Uncertainty, %
^{47}Sc on NaCl coated Al foil	3600	8128 ± 890	10.95
^{47}Sc liquid fraction	7200	6171 ± 684	11.09
Empty Al foil	7200	372 ± 77	20.70
Diba Omnifit EZ column 5 mm diameter	7200	x	x

Calculating **the radiochemical recoverability gives 75.9 ± 11.8 %.** As in the first ^{47}Sc separation, no activity was discovered in the column or other parts of the system, feedthrough, and wash fractions, however, **6 % has remained in the Al foil** giving **actual recoverability of ~ 94 %.** Disregarding the amount of ^{47}Sc left in the Al foil gives **recoverability upwards of 99.9 %.**

The elution profile of ^{47}Sc was measured using ThermoScientific FH 40G-L10 radiameter (γ) and registered as a function of time (at a distance of 15 cm, partially shielded by sample holder). The flow rate was increased during the elution phase, however, both flow rate and radioactivity were registered simultaneously and are shown in Fig. 19.

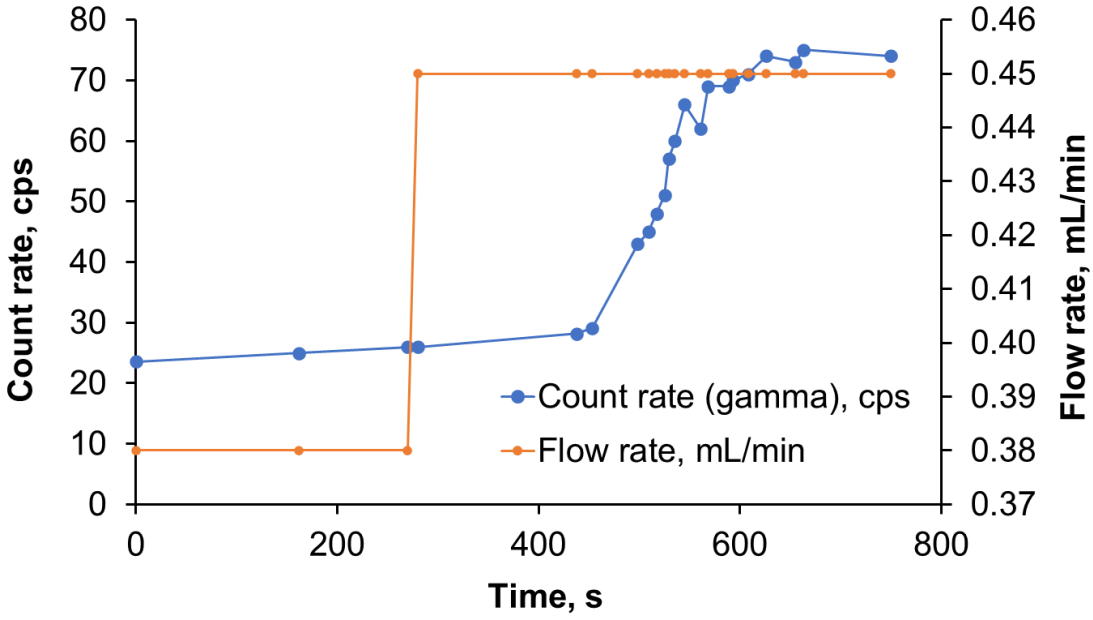

Fig. 19. **Elution profile for ^{47}Sc using gamma detector at 10 cm, partially shielded and the flow rate through the column**

By integrating the flow rate by time, it was found that the total volume of **0.1 M HCl in which all ^{47}Sc had eluted was 5 mL (saturation achieved in 3 mL).** Furthermore, the time for the **complete elution process took only 12 minutes.** The results are summarized in Fig. 20.

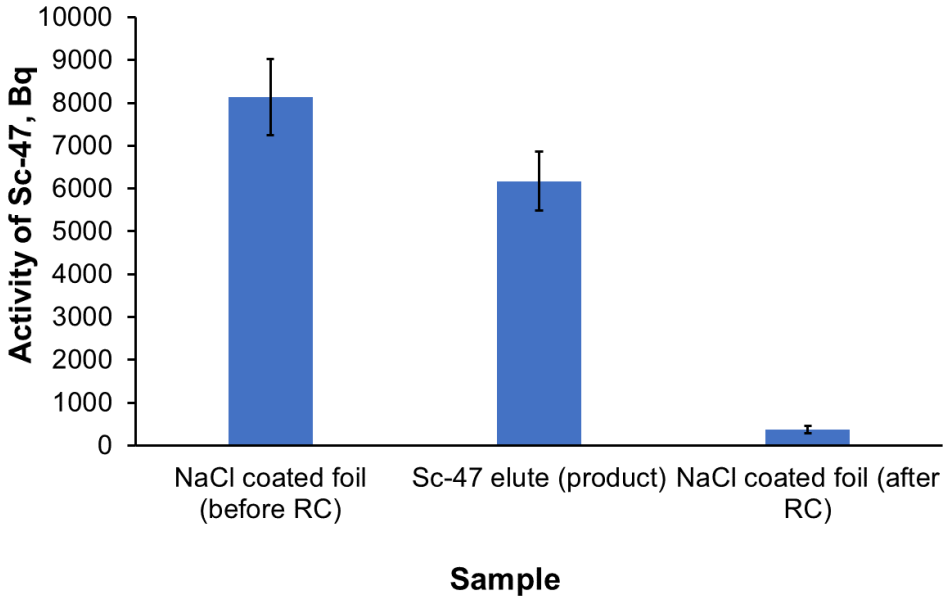

Fig. 20. **Gamma spectrometry results for the 2nd ^{47}Sc separation using ion-exchange chromatography, activity half-life corrected**

The whole separation process took **2.5 hours** including the setup of the system, column conditioning, disassembly, and system component monitoring for radioactive contamination.

CONCLUSIONS AND REMARKS

1. Electrochemical separation method shows application in contaminant removal (in aqueous solutions), however, is unsuitable for direct Sc removal in aqueous solutions;
2. Increased temperature or high ionic strength coupled with stirring at 600 rpm yielded the largest current and thus took the least amount of time;
3. Using a basic pump-assisted ion-exchange chromatography setup a ^{47}Sc separation **recoverability of 81.4 ± 13.2 % for 3 mm Diba Omnifit Benchmark Microbore column** has been achieved;
4. A semi-automated ion-exchange chromatography setup has been created and tested using ^{47}Sc achieving radiochemical separation **recoverability 75.9 ± 11.8 % for 5 mm Diba Omnifit EZ adjustable end-piece column**;
5. Since no activity was discovered elsewhere in the setup and other process liquids, the **actual radiochemical recoverability can be estimated to be ~ 99.9 %** (~ 95% if accounting for 5 - 6% left in Al foil bulk due to implantation);
6. A proposed schematic for a fully automized system has been shown;
7. Further research needed for Sc complete separation using electrochemical method for non-aqueous solutions.

ACKNOWLEDGEMENTS

The author of this report would like to personally thank CERN staff and especially Thierry Stora, Edgars Mamis, Laura N. Lambert, Charlotte Duchemin, Inzamam Muhammad, Bernard Crepieux and Mathieu Bovigny for supervision, suggestions, performing measurements, and aid in material procurement.

REFERENCES

[1] PRISMAP Consortium, PRISMAP Medical Radionuclide information site, (2023).

[2] B. Singh, J. Chen, Nuclear Data Sheets for A = 43, Nuclear Data Sheets. (2015) l1–150. https://doi.org/DOI:101016/jnds201505001.

[3] J. Chen, B. Singh, J.A. Cameron, Nuclear Data Sheets for A = 44, Nucl. Data Sheets. 112 (2011) 2357–2495. https://doi.org/10.1016/j.nds.2011.08.005.

[4] M.L. Halbert, Nuclear data sheets for A = 47, Nucl. Data Sheets. 22 (1977) 59–133. https://doi.org/10.1016/S0090-3752(77)80039-2.

[5] Y. Martinez Palenzuela, V. Barozier, E. Chevallay, T.E. Cocolios, C. Duchemin, P. Fernier, M. Huyse, L. Lambert, R. Lopez, S. Marzari, J.P. Ramos, T. Stora, P. Van Duppen, A. Vorozhtsov, The CERN-MEDICIS Isotope Separator Beamline, Front Med (Lausanne). 8 (2021). https://doi.org/10.3389/fmed.2021.689281.

[6] E. Lopienska, The CERN accelerator complex, layout in 2022. Complexe des accélérateurs du CERN en janvier 2022, (2022).

[7] E. Mamis, MEDICIS Collection and Operation report on MED-015 741M Ti target, Geneva, 2021.

[8] P. Vanýsek, Electrochemical Series, in: CRC Handbook of Chemistry and Physics (92nd Ed.), 92nd Edition, CRC Press, 2011: pp. 5–80.

[9] A. Raveendran, M. Chandran, R. Dhanusuraman, A comprehensive review on the electrochemical parameters and recent material development of electrochemical water splitting electrocatalysts, RSC Adv. 13 (2023) 3843–3876. https://doi.org/10.1039/D2RA07642J.

[10] M. Rasoulis, D. Vernardou, Electrodeposition of Vanadium Oxides at Room Temperature as Cathodes in Lithium-Ion Batteries, Coatings. 7 (2017). https://doi.org/10.3390/coatings7070100.

[11] M.E. Sibert, M.A. Steinberg, Electrodeposition of Titanium on Base Metals, J Electrochem Soc. 102 (1955) 641. https://doi.org/10.1149/1.2429928.

[12] P.P. Kumbhar, C.D. Lokhande, Electrodeposition of yttrium from a nonaqueous bath, Metal Finishing. 93 (1995) 28–31. https://doi.org/https://doi.org/10.1016/0026-0576(95)95843-6.

[13] H. Nulwala, J.D. Watkins, X. Zhou, Electrochemical Deposition of Elements in Aqueous Media, CA3009779, 2017.

[14] V.M. Prida, V. Vega, J. García, L. Iglesias, B. Hernando, I. Minguez-Bacho, 1 - Electrochemical methods for template-assisted synthesis of nanostructured materials, in: M. Vázquez (Ed.), Magnetic Nano- and Microwires, Woodhead Publishing, 2015: pp. 3–39. https://doi.org/https://doi.org/10.1016/B978-0-08-100164-6.00001-1.

[15] G. Alyward, T. Findlay, SI Chemical Data, 6th Edition, 2008.

[16] D. Lide, CRC Handbook of Chemistry and Physics, 87th ed., American Chemical Society, 2007. https://doi.org/10.1021/ja069813z.

[17] N.N. Greenwood, A. Earnshaw, Chemistry of the Elements (2nd ed.), 2nd Edition, Butterworth-Heinemann, 1997.

[18] M. Örvös, V. Szabó, T. Poós, Rate of evaporation from the free surface of a heated liquid, Journal of Applied Mechanics and Technical Physics. 57 (2016) 1108–1117. https://doi.org/10.1134/S0021894416060195.

[19] A. Raveendran, M. Chandran, R. Dhanusuraman, A comprehensive review on the electrochemical parameters and recent material development of electrochemical water splitting electrocatalysts, RSC Adv. 13 (2023) 3843–3876. https://doi.org/10.1039/D2RA07642J.

[20] Honeywell, Hydrogen lower explosive limit, (2023). https://sps-support.honeywell.com/s/article/What-is-the-equivalent-reading-of-Hydrogen-LEL-to-PPM (accessed September 7, 2023).

[21] Engineering Toolbox, Chlorine solubility in water, (2023). https://www.engineeringtoolbox.com/gases-solubility-water-d_1148.html (accessed September 7, 2023).

[22] E. Lundanes, L. Reubsaet, T. Greibrokk, General Concepts, in: Chromatography: Basic Principles, Sample Preparations and Related Methods, First Edition, Wiley-VCH Verlag GmbH & Co. KGaA, 2014.

[23] H.U. Khan, The Role of Ion Exchange Chromatography in Purification and Characterization of Molecules, in: A. Kilislioğlu (Ed.), Ion Exchange Technologies, IntechOpen, Rijeka, 2012. https://doi.org/10.5772/52537.

[24] K. Kilian, Ł. Cheda, M. Sitarz, K. Szkliniarz, J. Choiński, A. Stolarz, Separation of 44Sc from Natural Calcium Carbonate Targets for Synthesis of 44Sc-DOTATATE, Molecules. 23 (2018). https://doi.org/10.3390/molecules23071787.

[25] C. Vyas, J. Park, S. Yang, Application of Extraction Chromatographic Techniques for Separation and Purification of Radiometals Sc-44,47 and Cu-64, 67, Journal of Radiopharmaceuticals and Molecular Probes. 2 (2016) 84–95.

[26] M. Antonio, E. Horwitz, An europium(III) diglycolamide complex: insights into the coordination chemistry of lanthanides in solvent extraction, Dalton Trans. 44 (2014). https://doi.org/10.1039/C4DT01775G.

[27] V. Radchenko, C.A.L. Meyer, J.W. Engle, C.M. Naranjo, G.A. Unc, T. Mastren, M. Brugh, E.R. Birnbaum, K.D. John, F.M. Nortier, M.E. Fassbender, Separation of 44Ti from proton irradiated scandium by using solid-phase extraction chromatography and design of 44Ti/44Sc generator system, J Chromatogr A. 1477 (2016) 39–46. https://doi.org/https://doi.org/10.1016/j.chroma.2016.11.047.

[28] C. Dirks, T. Dirks, S. Happel, On the separation of Sc, Zr and Ga, Marburg and Bruz, 2022.

[29] P. Kalnina, Chemical Separation and Purification of Stable ^{45}Sc From The CERN-MEDICIS Mass-Separator Collection Foils, Geneva, 2022.

[30] M. Tabrizchi, F. Rouholahnejad, Comparing the effect of pressure and temperature on ion mobilities, J Phys D Appl Phys. 38 (2005) 857. https://doi.org/10.1088/0022-3727/38/6/012.

[31] M.M.E. Duarte, A.S. Pilla, J.M. Sieben, C.E. Mayer, Platinum particles electrodeposition on carbon substrates, Electrochem Commun. 8 (2006) 159–164. https://doi.org/https://doi.org/10.1016/j.elecom.2005.11.003.

[32] J.S. Noh, N.J. Laycock, W. Gao, D.B. Wells, Effects of nitric acid passivation on the pitting resistance of 316 stainless steel, Corros Sci. 42 (2000) 2069–2084. https://doi.org/https://doi.org/10.1016/S0010-938X(00)00052-4.

[33] Fisher Scientific, Diba Omnifit Benchmark Microbore Chromatography columns 3 mm, (2023). https://www.fishersci.com/shop/products/omnifit-benchmark-microbore-chromatography-columns-4/p-4675163#?keyword=diba%20omnifit%203mm (accessed September 7, 2023).

[34] J.D. Watkins, X. Zhou, H.B. Nulwala, (Invited) Aluminum Layer Electrodeposition from Aqueous Solutions, ECS Meeting Abstracts. MA2017-02 (2017) 989–989. https://doi.org/10.1149/MA2017-02/20/989.

[35] J.J. Parus, J. Kierzek, B. Malozewska-Bucko, Preliminary Results of Carbon Content Determination in Coal by XRF, Nucleonic Control Systems. (1998) 116.

[36] Inc. XRF Research, XRF spectrum for Ti, (2023). http://www.xrfresearch.com/xrf-spectrum-titanium/ (accessed September 7, 2023).